AD_____

Award Number: W81XWH-12-1-0604

TITLE: Deciphering the Adaptive Immune Response to Ovarian Cancer

PRINCIPAL INVESTIGATOR:

Brad H. Nelson, Ph.D.

CONTRACTING ORGANIZATION:

British Columbia Cancer Agency

Victoria BC V8R 6V5
Canada

REPORT DATE:

October 2014

TYPE OF REPORT:

Annual

PREPARED FOR: U.S. Army Medical Research and Materiel Command
Fort Detrick, Maryland 21702-5012

REPORT DOCUMENTATION PAGE

Form Approved
OMB No. 0704-0188

1. REPORT DATE *(DD-MM-YYYY)*	2. REPORT TYPE	3. DATES COVERED *(From - To)*
October 2014	Annual Report	Sept 30, 2013- Sept 29, 2014

4. TITLE AND SUBTITLE
Deciphering the Adaptive Immune Response to Ovarian Cancer

5a. CONTRACT NUMBER

5b. GRANT NUMBER
W81XWH-12-1-0604

5c. PROGRAM ELEMENT NUMBER

6. AUTHOR(S)
Brad H. Nelson, Ph.D.

email: bnelson@bccancer.bc.ca

5d. PROJECT NUMBER

5e. TASK NUMBER

5f. WORK UNIT NUMBER

7. PERFORMING ORGANIZATION NAME(S) AND ADDRESS(ES)

British Columbia Cancer
Agency,
2410 Lee Avenue,
Victoria BC V8R 6V5
Canada

8. PERFORMING ORGANIZATION REPORT NUMBER

9. SPONSORING / MONITORING AGENCY NAME(S) AND ADDRESS(ES)
US Army Medical Research and
Materiel Command
Fort Detrick, Maryland
21702-5012

10. SPONSOR/MONITOR'S ACRONYM(S)

11. SPONSOR/MONITOR'S REPORT NUMBER(S)

12. DISTRIBUTION / AVAILABILITY STATEMENT
Approved for public release; distribution unlimited

13. SUPPLEMENTARY NOTES

14. ABSTRACT The presence of CD8+ tumor-infiltrating lymphocytes (CD8+ TIL) has been associated with increased patient survival in ovarian cancer. We discovered that this effect is even stronger when CD8+ TIL are found together with CD20+ B cells and CD4+FoxP3+ T cells. We hypothesized that CD20+ TIL contribute to tumor immunity by presenting antigens to CD4+ and CD8+ TIL. This year, we discovered that the major antibody-producing cells in ovarian cancer are not CD20+ TIL but plasma cells, therefore our immunoglobulin cloning efforts are being directed toward these cells. We also discovered an unexpectedly high diversity of T cell receptors (TCR) among tumor-infiltrating T cells, which has prompted us to develop a new high throughput method for T cell antigen discovery. Finally, we discovered a novel subset of CD4+ T cells that is strongly associated with patient survival and will be the focus of future antigen identification efforts. Overall, this project is progressing on schedule and is yielding innovative methods and publishable results that lead toward a better understanding of the immune response to ovarian cancer.

15. SUBJECT TERMS
Tumor immunology, immunotherapy, ovarian cancer, antibody, T cell, tumor antigen

16. SECURITY CLASSIFICATION OF:			17. LIMITATION OF ABSTRACT	18. NUMBER OF PAGES	19a. NAME OF RESPONSIBLE PERSON
a. REPORT	b. ABSTRACT	c. THIS PAGE			USAMRMC
U	U	U	UU	64	19b. TELEPHONE NUMBER *(include area code)*

Table of Contents

W81XWH-12-1-0604 (OC110435) Annual Report, Oct 2014

PI: Brad H. Nelson, Ph.D.
Co-PIs: Rob Holt, Ph.D., John Webb Ph.D., Peter Watson, M.D.

Title of Project: Deciphering the Adaptive Immune Response to Ovarian Cancer

INTRODUCTION:

Tumor-infiltrating CD8+ T cells are strongly associated with increased survival in ovarian cancer. However, they do not work in isolation. We discovered that two other types of immune cell play an important supportive role: B cells and helper T cells (specifically, helper T cells that express a protein called FoxP3). We made this discovery by performing a systematic analysis of immune cells in ovarian cancer. We found that killer T cells are often found in small clusters together with B cells and helper T cells. Importantly, we found that patients whose tumors have these combinations of immune cells have better survival rates than patients whose tumors contain killer T cells alone. This tells us that T cells and B cells work together to attack tumors. These findings have powerful clinical implications: to enhance the immune response to ovarian cancer, we need to enhance the activity of all three types of immune cell, rather than killer T cells alone.

To explain these observations, we hypothesized that B cells serve as "organizers" that help to draw T cells into the tumor. In addition, B cells might present tumor proteins to the T cells to facilitate tumor recognition. We further hypothesized that FoxP3 helper T cells might produce cytokines that help to excite the killer T cells. To test these hypotheses, we proposed to determine which tumor proteins (antigens) are recognized by B cells and FoxP3 helper T cells in ovarian cancer. By identifying these antigens, we will be able to create new molecular tools to elucidate how the immune system recognizes and attacks ovarian cancer. The study has four tasks:

Task 1. To identify tumor antigens recognized by CD20+ TIL.

Task 2. To identify tumor antigens recognized by CD4+FoxP3+ TIL.

Task 3. To determine whether tumor-infiltrating B cells and T cells recognize the same antigens.

Task 4. To assess the functional phenotype of antigen-specific CD4+FoxP3+ TIL.

Significance: The immune system has a profound influence on survival from ovarian cancer. With better understanding of the immune response, it will be possible to design new treatments such as vaccines that enhance tumor immunity and increase patient survival. We envision our work will lead to a major re-think about cancer vaccines: instead of simply trying to activate killer T cells, we also need to find effective ways to activate their team mates, the B cells and FoxP3+ helper T cells.

BODY:

Task 1. To identify tumor antigens recognized by CD20+ TIL.

In this task, we proposed to identify the antigens recognized by the 3 most abundant CD20+ TIL clones from each of 3 ovarian cancer patients. To accomplish this, we proposed to clone immunoglobulin G (IgG) molecules from individual CD20+ TIL. These will be used to identify the corresponding antigens using three different approaches: candidate antigen assays, cDNA library screening, and mass spectrometry.

Progress to date:

As described in last year's report, we successfully developed methods based on single-cell sorting and PCR cloning to isolate matched IgG heavy and light chain sequences from CD20+ TIL. We focused on three HGSC cases for which the repertoire of IgG had previously been determined by Sanger sequencing of bulk tumor tissue. We sorted, cloned and expressed recombinant antibodies from over 30 single CD20+ TIL from these three tumors. Unexpectedly, none of the IgG sequences from single-sorted CD20+ B cells aligned to the dominant clonotypes determined by sequencing of bulk tumor tissue. Furthermore, we obtained no evidence of tumor reactivity on screening recombinant antibodies against HGSC cell lines. This puzzling result led to the hypothesis that the B cell component of TIL might be more heterogeneous than previously appreciated. We therefore turned to immunohistochemistry and flow cytometry to further investigate B-lineage cells in HGSC.

To this end, we performed multicolor immunohistochemistry on whole tumor sections from 21 HGSC patients. We found that CD20+ B cells often form dense aggregates with other lymphocytes within and around HGSC tumors **(Fig. 1)**. These aggregates resemble lymph nodes, yet are embedded within tumor tissue. Others have named these "ectopic lymphoid follicles" or "tertiary lymphoid structures" (TLS); we will use the latter designation. TLS appear to have all the components of normal lymph nodes. They have T cell zones containing CD4+ and CD8+T cells, activated dendritic cells expressing CD208, and high endothelial venules (HEVs). They also contain B cell-rich areas (called follicles), which contain interdigitating networks of follicular DCs, follicular helper T cells and germinal center B cells. We found the latter cells express the transcription factor Bcl-6 and activation-induced cytidine deaminase (AID), an enzyme involved in class-switch recombination and somatic hypermutation (not shown). Thus, TLS resemble lymph nodes in their organization, cellular composition, and ability to support immune reactions.

By flow cytometry, we found that the vast majority of tumor-infiltrating CD20+ B cells are IgG+ memory B cells. Most of these memory B cells appear to be activated (i.e., they express FAS) and express IgG. However, we also discovered that 9/10 cases contained an appreciable number of early plasma cells ($CD38^{high}$, $CD138^{low}$, IgD-). The proportion of these cells ranged from <5% to >80% of CD19+ cells. Importantly, these plasma cells do not express CD20 and therefore have been missed in previous immunohistochemical and sorting experiments. Plasma cells are known to express large amounts of IgG-encoding mRNA and protein. In fact, they are often referred to ask "antibody factories". Given this, we hypothesized that IgG sequencing from bulk tumor preparations might largely reflect the IgG repertoire of plasma cells. To address this, we used conventional FACS to isolate CD20+ TIL and $CD38^{high}$ plasma cells from tumor samples. We then sequenced the IgG repertoire in each sample and compared these sequences to those found in bulk tumor preparations from the same tumor. In 3/3 patients, we found that both CD20+ TIL and $CD38^{high}$ plasma cells are clonally expanded to some extent. We also found examples of shared IgG sequences between these two populations, suggesting that some CD20+ TIL are products of the same immune reactions that give rise to plasma cells. Importantly, we found that IgG sequences derived from plasma cells were highly over-represented in sequencing data from bulk tumor. Thus, we conclude that plasma cells in HGSC are the major source of clonally expanded IgG sequence and therefore are the more likely B lineage cell type to mediate anti-tumor immune reactions.

Having identified plasma cells as the major source clonally expanded B cell populations in HGSC, we are currently investigating the possibility that these cells are making antibodies to tumor-associated antigens. As per the original proposal, and last year's report, we are using single cell sorting followed by RT-PCR to molecularly clone matched IgG heavy and light chains from these cells. To date, we have isolated and PCR-cloned 6 matched IgG heavy and light

chain pairs derived from plasma cells from one HGSC patient. As expected, some of these antibodies correspond to clonally expanded populations dominating the IgG repertoire in both the plasma cell component and the bulk tumor (**Fig. 2**). We are currently expressing these cloned heavy and light chains as recombinant antibodies, which in turn will be screened for tumor reactivity. As per the original proposal, we will attempt to identify the antigens recognized by recombinant antibodies that react to tumor. In Task 3, we will assess whether T cells from the same tumor sample recognize these antigens.

Task 2. To identify tumor antigens recognized by CD4+FoxP3+ TIL.

We proposed to clone TCR molecules from CD4+FoxP3+ tumor-infiltrating T cells from the 3 ovarian cancer patients described above. Cloned TCR's will be expressed in a hybridoma cell line, which in turn will be used to identify the underlying antigens using a candidate approach and/or cDNA library screening.

Progress to date:

We proposed to choose from ascites from each of 3 HGSC patients, the 3 most abundant and persistent CD4+FoxP3+ TIL clones as identified by TCR-seq analysis, and proceed to identify their cognate antigens. TCR-seq analysis was completed but gave the surprising result that ascites T-cells were highly heterogeneous; we did not find any examples of abundant, persistent T-cell clones that were present in all three samples from a given subject. If we had observed a small number of dominant clontypes it would have made sense to proceed with conventional cloning and antigen identification as described in our original proposal. Now, however, we are faced with high clonal diversity of tumor-associated T cells and the question remains as to what antigens these populations of T cells are recognizing. This prompted us to refocus our approach, and work towards developing a more powerful, high-throughput and unbiased method for T cell antigen discovery.

As we have discussed in recent review articles, It is well recognized that TCR-seq has opened a new window on T-cell repertoires, but T-cell antigen profiling capabilities have not kept pace (see references 1 and 8 under Reportable Outcomes). The problem lies in the enormous complexity of the pMHC/TCR interaction, due to differential peptide processing, MHC allelic variation, TCR somatic recombination, and the requirement for co-receptors (CD8 or CD4). The approach we are now pursuing leverages natural antigen presentation, the single-cell resolution of flow cytometry, and the power of Next Generation Sequencing (NGS) to find DNA sequences that encode antigens recognized by tumour-associated T cells. Briefly, our method involves the use of a granzyme-B (GzmB)-cleavable fluorescent reporter gene linked to a library of all possible peptide-encoding sequences, derived, for example, from tumor cDNA. The antigen and reporter sequence is delivered by lentiviral gene transfer into seromatched antigen presenting cells in the form of an autologous, lymphoblastic cell line. Transduced target cells that receive a dose of GzmB from co-cultured cytolytic T cells of interest can be detected via cleavage of the encoded reporter protein and isolated by FACS. The identity of the epitopes carried by the marked cells are then determined by sequencing. This method has now been reduced to practice using the model antigen ovalbumen and cytolytic ovalbumen-specific T-cells from OT-I TCR-transgenic mice. Our next steps are to apply this approach to detecting cognate antigens from tumor cDNA from the ovariant cancer subjects studied here. We are starting by evaluating CD8+ cytolytic T cells from patient ascites, and we will subsequently modify the system to enable screening of TCRs of interest, identified by TCR-seq and transduced into CD8+ and CD4+ cytolytic T cell hybridomas, as described in our original proposal. Thus, we are adapting to new challenges presented by our project by developing and implementing novel solutions that will enable follow-on studies by ourselves and other investigators in this area.

Task 3. To determine whether tumor-infiltrating B cells and T cells recognize the same antigens.

Once we have identified cognate antigens for the predominant CD8+ (from the original IDEA proposal), CD20+ (Task 1) and CD4+FoxP3+ (Task 2) TIL, we proposed to assess the extent to which these antigen sets overlap. If the antigens recognized by CD20+ TIL are also recognized by CD8+ or CD4+ TIL, this would support our hypothesis that CD20+ TIL can serve as APC in the tumor environment.

Progress to date:

This task cannot start until Tasks 1 and 2 are completed, which is expected this year.

Task 4. To assess the functional phenotype of antigen-specific CD4+FoxP3+ TIL.

CD4+FoxP3+ TIL show great functional heterogeneity in EOC, which makes it difficult to draw definitive conclusions about their role in the tumor environment. With knowledge of their cognate antigens, we will be able to clarify this issue by assessing the functional phenotype of individual CD4+FoxP3+ T cell clones as opposed to bulk cell preparations. We proposed to do this by constructing MHC class II tetramers, which bind specifically to CD4+ T cells expressing TCRs relevant to a particular antigen.

Progress to date:

In flow cytometry experiments, we discovered that CD4+FoxP3+ TIL comprised two distinct populations that could be distinguished by their expression of CD25 (**Fig. 3**). In fact, the entire CD4+ TIL compartment could be subdivided into four subpopulations based on expression of FoxP3 and CD25 (**Fig. 3**). We performed additional flow cytometry experiments to assess the activation status and cytokine production profiles of these four CD4+ TIL subsets (n = 6 cases). CD25+FoxP3+ TIL had a classic regulatory T cell phenotype (**Fig. 3**). Unexpectedly, we discovered that the CD25+FoxP3- TIL subpopulation had a previously undescribed phenotype. On the one hand, they had an activated phenotype as evidenced by high CD69 and low CCR7 expression (not shown). In comparison to Tregs, CD25+FoxP3- TIL expressed similar levels of GITR; however, they expressed lower levels of CTLA-4 and OX40 and were negative for Helios (**Fig. 3**). These data suggested that CD25+FoxP3- cells might be Th1 cells, which are widely reported among TIL. However, CD25-+FoxP3- T cells failed to produce any of the hallmark Th1 cytokines IFN-γ, TNF-α or IL-2 after *in vitro* stimulation with PMA and ionomycin (**Fig. 3C**). Indeed, Th1 cytokines were only produced by the CD25-FoxP3- subset (**Fig. 3C**). None of the CD4+ TIL subsets produced IL-4 or IL-17A (not shown).

Given that CD25+FoxP3- T cells did not express canonical Th cytokines, we investigated the possibility that they might represent other less common CD4+ T cell phenotypes. CD4+ cytolytic T cells have been described in cancer; however, similar to other non-Treg cells, very few CD25+FoxP3- T cells expressed the cytolytic markers TIA-1, granzyme B or perforin (not shown). Furthermore, CD25+FoxP3- TIL did not express CXCR5, a marker of T follicular helper cells (not shown).

Based on their lack of discernible functional attributes, we hypothesized that CD25+FoxP3-TIL might be in a suppressed or exhausted state. In accord with this, we found that CD25+FoxP3- T cells expressed very high levels of the exhaustion marker PD-1 (**Fig. 3D**). Indeed, the level of PD-1 expressed by CD25+FoxP3- TIL was on average 3.1-fold higher than Tregs, and 6.6-fold higher than CD25-FoxP3- cells. In addition, CD25+FoxP3- TIL expressed the exhaustion markers LAG-3 (not shown) and TIM-3, the

latter being found on cells with the highest PD-1 levels (**Fig. 3D**). Thus, CD25+FoxP3- TIL exhibited an exhausted phenotype based on the expression of these markers and deficient cytokine production.

To investigate the prognostic significance of TIL subsets, a 187-case HGSC TMA was stained with antibodies to CD8, CD25 and FoxP3 (**Fig. 4**). Because CD4 is also expressed by macrophages, it is difficult to score CD4+ TIL directly. Instead, we assumed that any CD25+ and/or FoxP3+ cell that did not express CD8 was a CD4+ T cell, an assumption that was justified by flow cytometry (not shown). With this staining combination, we could directly visualize all CD8+ TIL subsets, as well as the CD25+FoxP3-, CD25+FoxP3+ and CD25-FoxP3+ subsets of CD4+ TIL. To infer the number of CD4+CD25-FoxP3- TIL, we employed a second IHC combination involving antibodies to CD3, CD8 and FoxP3. We determined the number of CD4+FoxP3- cells, which appeared as CD3+CD8-FoxP3- cells. From this, we subtracted the number of CD25+FoxP3- cells determined from the first staining combination. This yielded an estimate of the number of CD4+CD25-FoxP3- cells. Our detection and scoring approach proved valid, as the results obtained by multi-color IHC and flow cytometry were concordant. We stained an adjacent section of the TMA for cytokeratin to unequivocally identify tumor epithelium versus stroma; for all subsequent analyses we focused on intraepithelial TIL, as these have the greatest prognostic significance.

As expected, CD8+ TIL were strongly associated with disease-specific survival (HR = 0.33, P-value<0.0001; not shown) and progression free survival (HR = 0.38, P-value<0.0001) (**Fig. 4A**). The strong prognostic effect of CD8+ TIL can confound the analysis of closely associated TIL subsets, such as Tregs. Therefore, to determine the prognostic significance of CD4+ TIL subsets, we restricted our analysis to cases that were positive for CD8+ TIL. As expected, cases with a higher than median ratio of Tregs to CD8+ TIL trended toward decreased survival (HR = 1.55, P-value=0.09) (**Fig. 4B**). In contrast, a higher than median ratio of CD25+FoxP3- TIL to CD8+ TIL was strongly associated with survival (HR = 0.56, P-value=0.02) (**Fig. 4C**). The prognostic effect of CD25+FoxP3- TIL was even more pronounced in cases with lower levels of Tregs (HR = 0.29, P-value=0.003) (**Fig. 4D**). No other CD4+ TIL subsets showed an association with survival (not shown). Thus, the CD25+FoxP3- subset was unique among CD4+ TIL in showing a positive association with patient survival.

Thus, we have discovered a novel subset of CD4+ TIL that, like FoxP3+ TIL, express the activation marker CD25. Importantly, however, whereas CD25+FoxP3+ TIL are associated with poor prognosis (consistent with them being Tregs), CD25+FoxP3- T cells are associated with favorable prognosis. We now believe that these cells are responsible for the favorable prognosis that we previously attributed to FoxP3+ TIL. Thus, in Task 3 we intend to focus our antigen discovery efforts on this subset of CD4+ TIL. As for Task 4, a manuscript describing the above findings is “conditionally accepted” by the AACR journal *Cancer Immunology Research* **(Appendix B),** therefore we consider Task 4 to be completed.

KEY RESEARCH ACCOMPLISHMENTS:

1) We published a key manuscript describing the results of the original IDEA award:

   Wick, D., Webb, J.R., Nielsen, J.S., Martin, S., Kroeger, D.R., Milne, K., Castellarin, M., Twumasi-Boateng, K., Watson, P.H., Holt, R.H., Nelson, B.H. 2014. Surveillance of the tumor mutanome by T cells during progression from primary to recurrent ovarian cancer.

Clin Cancer Res. Mar 1;20(5):1125-34. Epub 2013 Feb 7. PMID: 24323902. ***(Appendix A)***

2) We submitted a key manuscript describing our discovery of a prognostically favorable CD4+ T cell subset in ovarian cancer:

   deLeeuw, R.D., Kroeger, D.R., Kost, S.E., Chang, P.-P., Webb, J.R., **Nelson, B.H.** 2014. CD25 identifies a subset of CD4+FoxP3-TIL that are exhausted yet prognostically favorable in human ovarian cancer. "*Conditionally accepted" by Cancer Immunology Research. **(Appendix B)***

3) As listed below, in 2012-2013 our team published 8 other manuscripts with direct relevance to this project, and 16 with indirect relevance.

4) Task 1: We discovered that the bulk of IgG sequences from tumors are derived from plasma cells, so our IgG cloning efforts are now directed toward these cells instead of CD20+ B cells.

5) Task 1: Robust methods have been developed to amplify matched IgG heavy and light chains by single-cell RT-PCR, to clone CDR3 regions into IgG expression vectors, and to prepare recombinant IgG.

6) Task 2: Faced with an unexpectedly high diversity of TCR sequences among TIL, we are developing an entirely new high throughput method to identify the antigens recognized by TIL. This method will be applicable to not only this project, but many future projects by us and others.

7) Task 4: This task was completed in 2013/2014. A manuscript describing the results is "conditionally accepted" by *Cancer Immunology Research* **(Appendix B).**

REPORTABLE OUTCOMES:

Manuscripts with direct relevance published by the team in 2013/2014 (n = 9):

1. Sharma G, **Holt RA**. T-cell epitope discovery technologies. Hum Immunol. 2014 Jun;75(6):514-9. doi: 10.1016/j.humimm.2014.03.003. Epub 2014 Apr 19. PubMed PMID: 24755351.
2. Brown SD, Warren RL, Gibb EA, Martin SD, Spinelli JJ, **Nelson BH, Holt RA**. Neo-antigens predicted by tumor genome meta-analysis correlate with increased patient survival. Genome Res. 2014 May;24(5):743-50. doi: 10.1101/gr.165985.113. Epub 2014 Apr 29. PubMed PMID: 24782321; PubMed Central PMCID: PMC4009604.
3. Wick DA, **Webb JR**, Nielsen JS, Martin SD, Kroeger DR, Milne K, Castellarin M, Twumasi-Boateng K, **Watson PH, Holt RA, Nelson BH**. Surveillance of the tumor mutanome by T cells during progression from primary to recurrent ovarian cancer. Clin Cancer Res. 2014 Mar 1;20(5):1125-34. doi: 10.1158/1078-0432.CCR-13-2147. Epub 2013 Dec 9. PubMed PMID: 24323902.
4. **Webb JR**, Milne K, **Watson P**, Deleeuw RJ, **Nelson BH**. Tumor-infiltrating lymphocytes expressing the tissue resident memory marker CD103 are associated with increased survival in high-grade serous ovarian cancer. Clin Cancer Res. 2014 Jan 15;20(2):434-44. doi: 10.1158/1078-0432.CCR-13-1877. Epub 2013 Nov 4. PubMed PMID: 24190978.
5. **Webb JR**, Milne K, **Nelson BH**. Location, location, location: CD103 demarcates intraepithelial, prognostically favorable CD8(+) tumor-infiltrating lymphocytes in ovarian

cancer. Oncoimmunology. 2014 Jan 10;3:e27668. eCollection 2014. PubMed PMID: 25101220; PubMed Central PMCID: PMC4121334.

6. Castellarin M, Milne K, Zeng T, Tse K, Mayo M, Zhao Y, **Webb JR, Watson PH, Nelson BH, Holt RA**. Clonal evolution of high-grade serous ovarian carcinoma from primary to recurrent disease. J Pathol. 2013 Mar;229(4):515-24. doi: 10.1002/path.4105. Epub 2012 Nov 29. PubMed PMID: 22996961.
7. West NR, Kost SE, Martin SD, Milne K, Deleeuw RJ, **Nelson BH, Watson PH**. Tumour-infiltrating FOXP3(+) lymphocytes are associated with cytotoxic immune responses and good clinical outcome in oestrogen receptor-negative breast cancer. Br J Cancer. 2013 Jan 15;108(1):155-62. doi: 10.1038/bjc.2012.524. Epub 2012 Nov 20. PubMed PMID: 23169287; PubMed Central PMCID: PMC3553524.
8. Woodsworth DJ, Castellarin M, **Holt RA**. Sequence analysis of T-cell repertoires in health and disease. Genome Med. 2013 Oct 30;5(10):98. doi: 10.1186/gm502. eCollection 2013. Review. PubMed PMID: 24172704; PubMed Central PMCID:PMC3979016.
9. Townsend KN, Spowart JE, Huwait H, Eshragh S, West NR, Elrick MA, Kalloger SE, Anglesio M, **Watson PH**, Huntsman DG, Lum JJ. Markers of T cell infiltration and function associate with favorable outcome in vascularized high-grade serous ovarian carcinoma. PLoS One. 2013 Dec 23;8(12):e82406. doi: 10.1371/journal.pone.0082406. eCollection 2013. PubMed PMID: 24376535; PubMed Central PMCID: PMC3871161.

Manuscripts with indirect relevance published by the team in 2013/2014 (n = 28):

1. Watson CT, Steinberg KM, Graves TA, Warren RL, Malig M, Schein J, Wilson RK, Holt RA, Eichler EE, Breden F. Sequencing of the human IG light chain loci from a hydatidiform mole BAC library reveals locus-specific signatures of genetic diversity. Genes Immun. 2014 Oct 23. doi: 10.1038/gene.2014.56. [Epub ahead of print] PubMed PMID: 25338678.
2. Parfenov M, Pedamallu CS, Gehlenborg N, Freeman SS, Danilova L, Bristow CA, Lee S, Hadjipanayis AG, Ivanova EV, Wilkerson MD, Protopopov A, Yang L, Seth S, Song X, Tang J, Ren X, Zhang J, Pantazi A, Santoso N, Xu AW, Mahadeshwar H, Wheeler DA, Haddad RI, Jung J, Ojesina AI, Issaeva N, Yarbrough WG, Hayes DN, Grandis JR, El-Naggar AK, Meyerson M, Park PJ, Chin L, Seidman JG, Hammerman PS, Kucherlapati R; the Cancer Genome Atlas Network; the Cancer Genome Atlas Network. Characterization of HPV and host genome interactions in primary head and neck cancers. Proc Natl Acad Sci U S A. 2014 Oct 13. pii: 201416074. [Epub ahead of print] PubMed PMID: 25313082.
3. Barnes RO, Schacter B, Kodeeswaran S, Watson PH. Funding sources for Canadian biorepositories: the role of user fees and strategies to help fill the gap. Biopreserv Biobank. 2014 Oct;12(5):300-5. doi: 10.1089/bio.2014.0052. Epub 2014 Oct 14. PubMed PMID: 25314324.
4. Cancer Genome Atlas Research Network. Comprehensive molecular characterization of gastric adenocarcinoma. Nature. 2014 Sep 11;513(7517):202-9. doi: 10.1038/nature13480. Epub 2014 Jul 23. PubMed PMID: 25079317; PubMed Central PMCID: PMC4170219.
5. Davis CF, Ricketts CJ, Wang M, Yang L, Cherniack AD, Shen H, Buhay C, Kang H, Kim SC, Fahey CC, Hacker KE, Bhanot G, Gordenin DA, Chu A, Gunaratne PH, Biehl M, Seth S, Kaipparettu BA, Bristow CA, Donehower LA, Wallen EM, Smith AB, Tickoo SK, Tamboli P, Reuter V, Schmidt LS, Hsieh JJ, Choueiri TK, Hakimi AA; Cancer Genome Atlas Research Network, Chin L, Meyerson M, Kucherlapati R, Park WY, Robertson AG, Laird PW, Henske EP, Kwiatkowski DJ, Park PJ, Morgan M, Shuch B, Muzny D, Wheeler DA, Linehan WM, Gibbs RA, Rathmell WK, Creighton CJ. The somatic genomic landscape of chromophobe

renal cell carcinoma. Cancer Cell. 2014 Sep 8;26(3):319-30. doi: 10.1016/j.ccr.2014.07.014. Epub 2014 Aug 21. PubMed PMID: 25155756; PubMed Central PMCID: PMC4160352.

6. Matzke L, Dee S, Bartlett J, Damaraju S, Graham K, Johnston R, Mes-Masson AM, Murphy L, Shepherd L, Schacter B, Watson PH. A practical tool for modeling biospecimen user fees. Biopreserv Biobank. 2014 Aug;12(4):234-9. doi: 10.1089/bio.2014.0008. PubMed PMID: 25162459.
7. Cancer Genome Atlas Research Network. Comprehensive molecular profiling of lung adenocarcinoma. Nature. 2014 Jul 31;511(7511):543-50. doi: 10.1038/nature13385. Epub 2014 Jul 9. Erratum in: Nature. 2014 Oct 9;514(7521):262. Rogers, K [corrected to Rodgers, K]. PubMed PMID: 25079552.
8. Watson PH. Biobank classification: communicating biorepository diversity. Biopreserv Biobank. 2014 Jun;12(3):163-4. doi: 10.1089/bio.2014.1231. PubMed PMID: 24955732.
9. Braun L, Lesperance M, Mes-Massons AM, Tsao MS, Watson PH. Individual investigator profiles of biospecimen use in cancer research. Biopreserv Biobank. 2014 Jun;12(3):192-8. doi: 10.1089/bio.2013.0092. Epub 2014 Jun 11. PubMed PMID: 24918606.
10. McKinnon ML, Rozmus J, Fung SY, Hirschfeld AF, Del Bel KL, Thomas L, Marr N, Martin SD, Marwaha AK, Priatel JJ, Tan R, Senger C, Tsang A, Prendiville J, Junker AK, Seear M, Schultz KR, Sly LM, Holt RA, Patel MS, Friedman JM, Turvey SE. Combined immunodeficiency associated with homozygous MALT1 mutations. J Allergy Clin Immunol. 2014 May;133(5):1458-62, 1462.e1-7. doi: 10.1016/j.jaci.2013.10.045. Epub 2013 Dec 12. PubMed PMID: 24332264.
11. Cancer Genome Atlas Research Network. Comprehensive molecular characterization of urothelial bladder carcinoma. Nature. 2014 Mar 20;507(7492):315-22. doi: 10.1038/nature12965. Epub 2014 Jan 29. PubMed PMID: 24476821; PubMed Central PMCID: PMC3962515.
12. West NR, Murray JI, Watson PH. Oncostatin-M promotes phenotypic changes associated with mesenchymal and stem cell-like differentiation in breast cancer. Oncogene. 2014 Mar 20;33(12):1485-94. doi: 10.1038/onc.2013.105. Epub 2013 Apr 15. PubMed PMID: 23584474.
13. Watson PH, Nussbeck SY, Carter C, O'Donoghue S, Cheah S, Matzke LA, Barnes RO, Bartlett J, Carpenter J, Grizzle WE, Johnston RN, Mes-Masson AM, Murphy L, Sexton K, Shepherd L, Simeon-Dubach D, Zeps N, Schacter B. A framework for biobank sustainability. Biopreserv Biobank. 2014 Feb;12(1):60-8. doi: 10.1089/bio.2013.0064. PubMed PMID: 24620771; PubMed Central PMCID: PMC4150367.
14. de Leeuw CN, Dyka FM, Boye SL, Laprise S, Zhou M, Chou AY, Borretta L, McInerny SC, Banks KG, Portales-Casamar E, Swanson MI, D'Souza CA, Boye SE, Jones SJ, Holt RA, Goldowitz D, Hauswirth WW, Wasserman WW, Simpson EM. Targeted CNS Delivery Using Human MiniPromoters and Demonstrated Compatibility with Adeno-Associated Viral Vectors. Mol Ther Methods Clin Dev. 2014 Jan 8;1:5. PubMed PMID: 24761428; PubMed Central PMCID: PMC3992516.
15. Johnson LD, Nesslinger NJ, Blood PA, Chima N, Richier LR, Ludgate C, Pai HH, Lim JT, Nelson BH, Vlachaki MT, Lum JJ. Tumor-associated autoantibodies correlate with poor outcome in prostate cancer patients treated with androgen deprivation and external beam radiation therapy. Oncoimmunology. 2014 Jun 25;3:e29243. eCollection 2014. PubMed PMID: 25114831; PubMed Central PMCID: PMC4125379.

16. Schmouth JF, Castellarin M, Laprise S, Banks KG, Bonaguro RJ, McInerny SC, Borretta L, Amirabbasi M, Korecki AJ, Portales-Casamar E, Wilson G, Dreolini L, Jones SJ, Wasserman WW, Goldowitz D, Holt RA, Simpson EM. Non-coding-regulatory regions of human brain genes delineated by bacterial artificial chromosome knock-in mice. BMC Biol. 2013 Oct 14;11:106. doi: 10.1186/1741-7007-11-106. PubMed PMID: 24124870; PubMed Central PMCID: PMC4015596.

17. Sio A, Chehal MK, Tsai K, Fan X, Roberts ME, Nelson BH, Grembecka J, Cierpicki T, Krebs DL, Harder KW. Dysregulated hematopoiesis caused by mammary cancer is associated with epigenetic changes and hox gene expression in hematopoietic cells. Cancer Res. 2013 Oct 1;73(19):5892-904. doi: 10.1158/0008-5472.CAN-13-0842. Epub 2013 Aug 1. PubMed PMID: 23913828.

18. Cancer Genome Atlas Research Network, Weinstein JN, Collisson EA, Mills GB, Shaw KR, Ozenberger BA, Ellrott K, Shmulevich I, Sander C, Stuart JM. The Cancer Genome Atlas Pan-Cancer analysis project. Nat Genet. 2013 Oct;45(10):1113-20. doi: 10.1038/ng.2764. PubMed PMID: 24071849; PubMed Central PMCID: PMC3919969.

19. Yan Y, Li X, Blanchard A, Bramwell VH, Pritchard KI, Tu D, Shepherd L, Myal Y, Penner C, Watson PH, Leygue E, Murphy LC. Expression of both estrogen receptor-beta 1 (ER-β1) and its co-regulator steroid receptor RNA activator protein (SRAP) are predictive for benefit from tamoxifen therapy in patients with estrogen receptor-alpha (ER-α)-negative early breast cancer (EBC). Ann Oncol. 2013 Aug;24(8):1986-93. doi: 10.1093/annonc/mdt132. Epub 2013 Apr 11. PubMed PMID: 23579816.

20. Cheah S, O'Donoghue S, Daudt H, Dee S, LeBlanc J, Braun L, Barnes R, Vercauteren S, Boone RH, Watson PH. Permission to contact (PTC)--a strategy to enhance patient engagement in translational research. Biopreserv Biobank. 2013 Aug;11(4):245-52. doi: 10.1089/bio.2013.0023. PubMed PMID: 24845592.

21. Cancer Genome Atlas Research Network. Comprehensive molecular characterization of clear cell renal cell carcinoma. Nature. 2013 Jul 4;499(7456):43-9. doi: 0.1038/nature12222. Epub 2013 Jun 23. PubMed PMID: 23792563; PubMed Central PMCID: PMC3771322.

22. LeBlanc J, Dee S, Braun L, Daudt H, Cheah S, Watson PH. Impact of a Permission to Contact (PTC) platform on biobank enrollment and efficiency. Biopreserv Biobank. 2013 Jun;11(3):144-8. doi: 10.1089/bio.2013.0004. Epub 2013 May 31. PubMed PMID: 24850090.

23. Cancer Genome Atlas Research Network. Genomic and epigenomic landscapes of adult de novo acute myeloid leukemia. N Engl J Med. 2013 May 30;368(22):2059-74. doi: 10.1056/NEJMoa1301689. Epub 2013 May 1. Erratum in: N Engl J Med. 2013 Jul 4;369(1):98. PubMed PMID: 23634996; PubMed Central PMCID: PMC3767041.

24. Warren RL, Freeman DJ, Pleasance S, Watson P, Moore RA, Cochrane K, Allen-Vercoe E, Holt RA. Co-occurrence of anaerobic bacteria in colorectal carcinomas. Microbiome. 2013 May 15;1(1):16. doi: 10.1186/2049-2618-1-16. PubMed PMID: 24450771; PubMed Central PMCID: PMC3971631.

25. Cancer Genome Atlas Research Network, Kandoth C, Schultz N, Cherniack AD, Akbani R, Liu Y, Shen H, Robertson AG, Pashtan I, Shen R, Benz CC, Yau C, Laird PW, Ding L, Zhang W, Mills GB, Kucherlapati R, Mardis ER, Levine DA. Integrated genomic characterization of endometrial carcinoma. Nature. 2013 May 2;497(7447):67-73. doi: 10.1038/nature12113. Erratum in: Nature. 2013 Aug 8;500(7461):242. PubMed PMID: 23636398; PubMed Central PMCID: PMC3704730.

26. Watson CT, Steinberg KM, Huddleston J, Warren RL, Malig M, Schein J, Willsey AJ, Joy JB, Scott JK, Graves TA, Wilson RK, Holt RA, Eichler EE, Breden F. Complete haplotype sequence of the human immunoglobulin heavy-chain variable, diversity, and joining genes and characterization of allelic and copy-number variation. Am J Hum Genet. 2013 Apr 4;92(4):530-46. doi: 10.1016/j.ajhg.2013.03.004. Epub 2013 Mar 28. PubMed PMID: 23541343; PubMed Central PMCID: PMC3617388.

27. Le Page C, Köbel M, de Ladurantaye M, Rahimi K, Madore J, Babinszky S, Bachvarov DR, Bachvarova M, Beauchamp MC, Cass CE, Chadwick D, Colleen C, Damaraju S, Dufour J, Gotlieb WH, Kalloger SE, Portelance L, McAlpine JN, Matte I, Piché A, Shaw P, Roehrl MH, Vanderhyden BC, Watson PH, Huntsman DG, Provencher DM, Mes-Masson AM. Specimen quality evaluation in Canadian biobanks participating in the COEUR repository. Biopreserv Biobank. 2013 Apr;11(2):83-93. doi: 10.1089/bio.2012.0044. Erratum in: Biopreserv Biobank. 2013 Aug;11(4):257. Roehrl, Michael H A [added]. PubMed PMID: 24845429.

28. Branton WG, Ellestad KK, Maingat F, Wheatley BM, Rud E, Warren RL, Holt RA, Surette MG, Power C. Brain microbial populations in HIV/AIDS: α-proteobacteria predominate independent of host immune status. PLoS One. 2013;8(1):e54673. doi: 10.1371/journal.pone.0054673. Epub 2013 Jan 23. PubMed PMID: 23355888; PubMed Central PMCID: PMC3552853.

Leveraged funding:

In 2013/2014, we obtained three new grants that are directly relevant to ovarian cancer immunology/immunotherapy:

1. How does the immune system contend with intratumoral heterogeneity?
Source: Canadian Cancer Society Research Institute
Dates: 02/2014 – 01/2016 Term: 2 years
PI: **Brad Nelson**
Co-PIs: **Rob Holt** and Sohrab Shah
The major goal of this project is to understand how the immune system controls tumor progression despite the presence of multiple tumor lineages within ovarian cancer patients.

2. Mechanisms of protective immunity in ovarian cancer
Source: Canadian Institutes of Health Research (CIHR)
Dates: 10/2014 – 03/2015 Term: 1 year (bridge funding)
PI: **Brad Nelson**
The major goal of this project is to define the mechanisms by which tumor-infiltrating T cells and B cells work together to promote effective tumor immunity in the setting of high-grade serous ovarian cancer.

3. What proportion of mutations in the ovarian cancer genome can be recognized by the immune system?
Source: Cancer Research Society
Dates: 10/2014 – 09/2016 Term: 2 years
PI: **Brad Nelson**
The major goal of this project is to determine whether ovarian tumors express mutated antigens that can potentially be recognized by CD8+ T cells and targeted by immunotherapy.

We also obtained a fourth grant with indirect relevance to this project:

4. Mutant MYD88: A target for adoptive T cell therapy of WM
Source: The Waldenstrom's Macroglobulinemia Foundation of Canada and the International Waldenstrom's Macroglobulinemia Foundation (IWMF)
Dates: 10/2014 – 09/2016 Term: 2 years
PI: **Brad Nelson**
The major goal of this project is to develop and validate TCR contructs that will allow us to engineer CD8+ T cells to specifically recognize a common mutation in Waldenstrom's Macroglobulinemia (MYD88L265P).

CONCLUSION:

Overall, this study is progressing on schedule and on budget. We have developed the necessary methods to complete Tasks 1 and 2, which will enable progress to Task 3 this year. Task 4 has been completed and is conditionally accepted for publication. In 2013-2014, we published 9 manuscripts with direct relevance and 28 with indirect relevance. Additional funding (4 competitive grants) has been received from several other agencies, enhancing the strength of our cancer immunology research program.

APPENDICES:

A. Wick, D., Webb, J.R., Nielsen, J.S., Martin, S., Kroeger, D.R., Milne, K., Castellarin, M., Twumasi-Boateng, K., Watson, P.H., Holt, R.H., Nelson, B.H. 2014. Surveillance of the tumor mutanome by T cells during progression from primary to recurrent ovarian cancer. *Clin Cancer Res.* Mar 1;20(5):1125-34. Epub 2013 Feb 7. PMID: 24323902.

B. deLeeuw, R.D., Kroeger, D.R., Kost, S.E., Chang, P.-P., Webb, J.R., **Nelson, B.H.** 2014. CD25 identifies a subset of CD4+FoxP3-TIL that are exhausted yet prognostically favorable in human ovarian cancer. "*Conditionally accepted" by Cancer Immunology Research.*

REFERENCES:

N/A

SUPPORTING DATA:

None.

FIGURES:

See following pages.

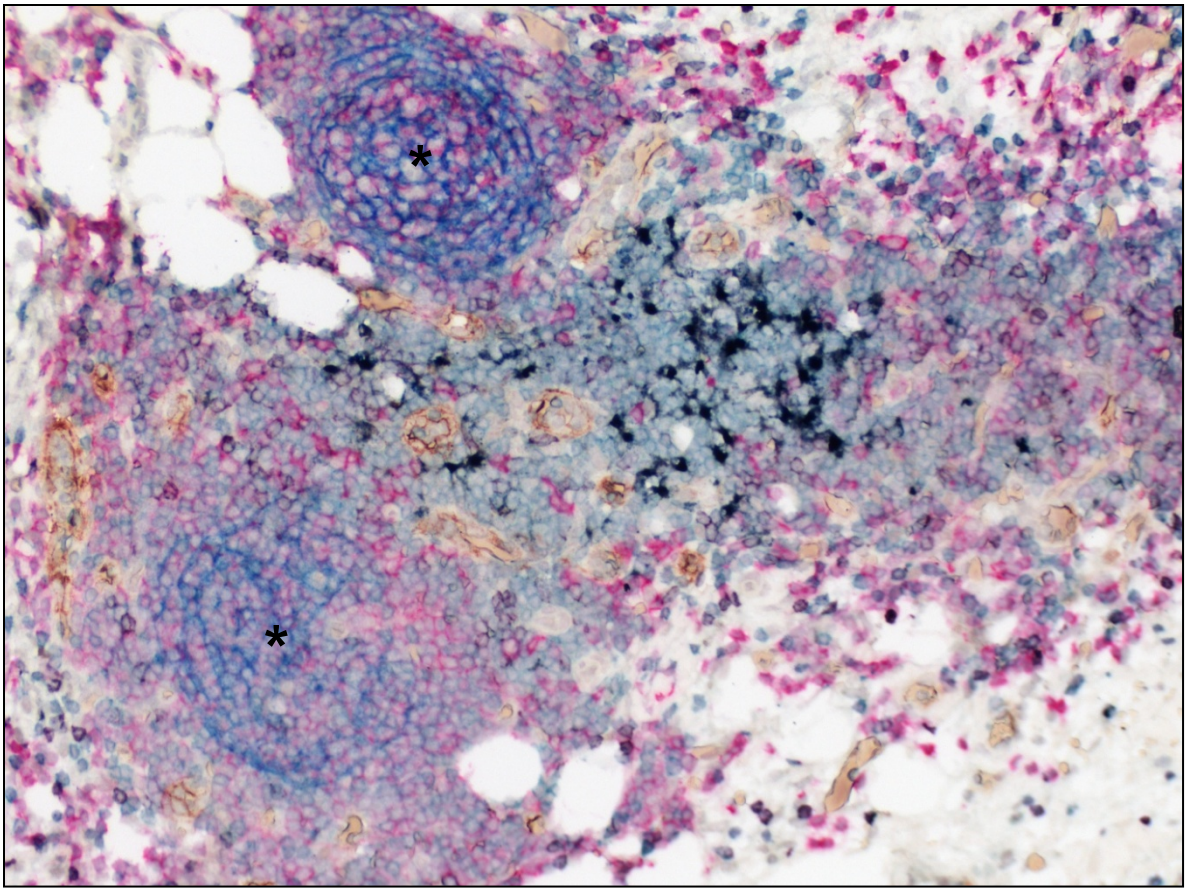

Figure 1. Tertiary lymphoid structures (TLS) in HGSC. Six-color immunohisto-chemistry was performed on a whole section from an HGSC tumor, revealing an example of a well organized lymph node-like structure termed a TLS. Shown are two B cell follicles (marked with *) containing CD20+ (red) B cells and interdigitating networks of CD21+ follicular dendritic cells (blue). Adjacent T cell zones are occupied by CD4+ T cells (blue-green), CD8+ T cells (purple), and CD208+ activated dendritic cells (black). The T cell zones also contain high endothelial-like venules (HEVs) bearing peripheral node addressins (brown), which recruit lymphocytes from the blood.

Significance to the project: This data is relevant to Tasks 1 and 3, as experiments such as this have given us unprecedented insight into the diversity of the B cell compartment in HGSC. As described in the annual report, we initially intended to isolate IgG molecules from CD20+ B cells, but we now realize the more prevalent and important IgG molecules are produced by plasma cells originating from tumor-associated TLS such as this.

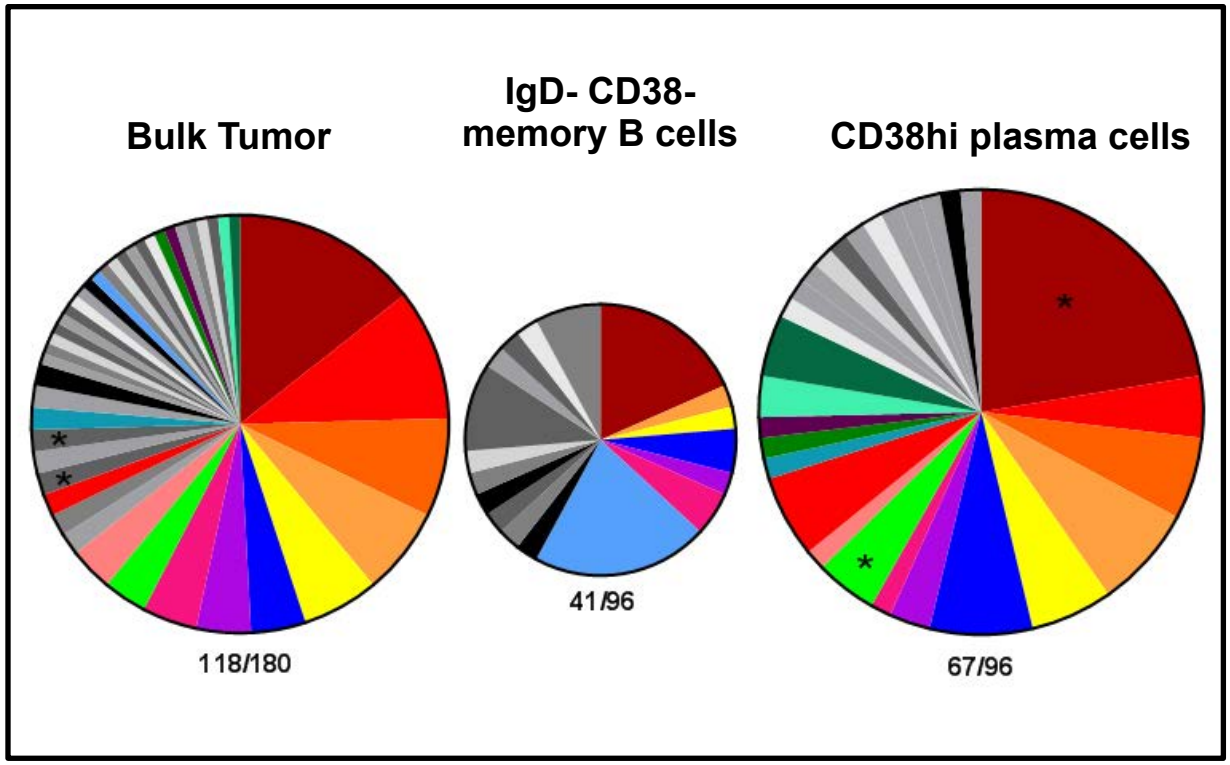

Figure 2. Clonal distribution of immunoglobulin (IgG) heavy chain sequences from different B lineage compartments found in HGSC. A single disaggregated HGSC sample was divided into three fractions. First, an unselected fraction (Bulk Tumor, *left*) was prepared. Second, FACS was used to sort IgD-negative CD38-negative memory B cells (*center*) and IgD-negative CD38-high plasma cells (*right*) from the remaining sample. mRNA was prepared from each of the three cell populations and converted to cDNA. IgG heavy chain-encoding cDNA was PCR-amplified from each of the fractions. PCR products were directionally cloned into a plasmid vector and used to transform *E. coli*. Transformed *E. coli* were plated onto selection media, and the resulting colonies were picked, screened for the presence of insert, and Sanger sequenced using IgG-specific sequencing primers. The number of IgG-positive colonies is shown below each of the three pie graphs, and is further represented by the size of the pie graph. Colored pie slices indicate IgG sequences that are shared between populations. Gray-scale slices indicate IgG sequences that were observed only in one cell population. The size of each piece represents the number of unique, yet clonally related, sequences observed. Asterisks (*) indicate IgG heavy chains that have been successfully molecularly cloned (both heavy and light chains) from individual plasma cells sorted from disaggregated tumor from the same patient.

Significance to the project: This data is relevant to Tasks 1 and 3. It demonstrates that plasma cells (*right*) give rise to the majority of abundant IgG sequences in bulk tumor preparations. In the next year, a similar cell sorting strategy as that shown on the right will be used to isolate additional plasma cells and molecularly clone their corresponding IgG molecules. As described in the original proposal, recombinant IgG molecules will then be used to identify the tumor-associated antigens recognized by these antibodies.

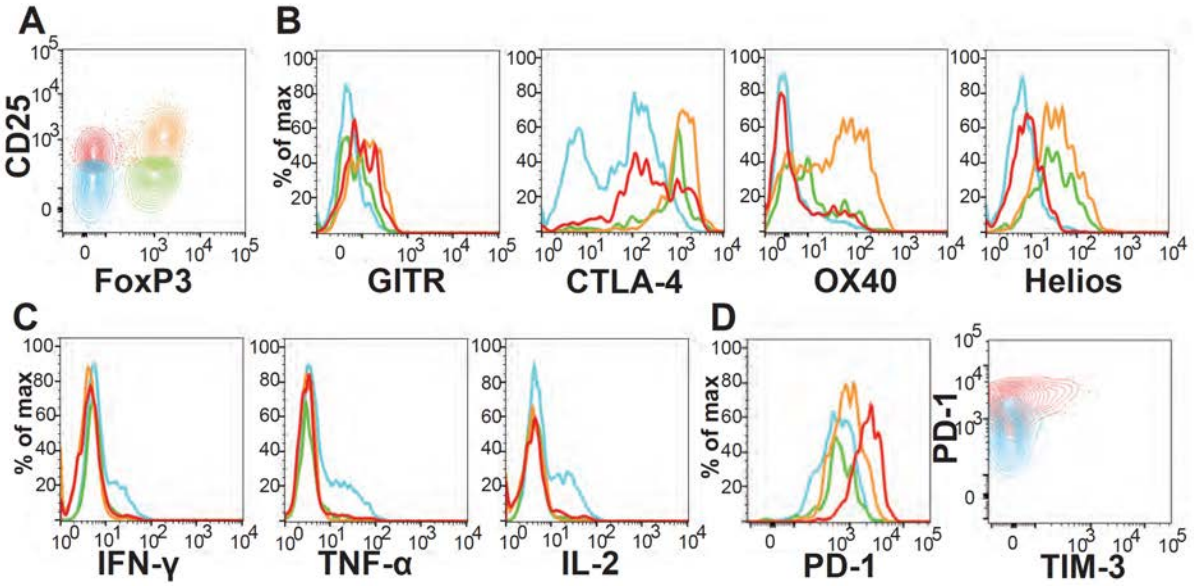

Figure 3. Phenotype and functional characteristics of CD4+ TIL subsets. Multi-parameter flow cytometry was used to assess expression of the indicated activation and differentiation markers and cytokines for four CD4+ T cell subsets defined by CD25 and FoxP3 expression. **(A)** Contour plot showing four CD4+ TIL subsets and color scheme used in other panels: CD25+FoxP3- (red), CD25+FoxP3+ (orange), CD25-FoxP3- (blue), CD25-FoxP3+ (green). **(B)** Expression of T cell activation and differentiation markers by the four TIL subsets. **(C)** Cytokine production after 3 hours of stimulation with PMA and ionomycin. **(D)** Expression of exhaustion markers (note that the right panel shows only the CD25+FoxP3- and CD25-FoxP3- subsets). Data is shown for one representative case from a total of six. Additional information can be found in deLeeuw et al. **(Appendix B)**.

Significance to the project: This data is relevant to Task 4. It demonstrates that CD4+CD25+FoxP3+ T cells have a classic regulatory T cell (Treg) phenotype. It also identifies a previously under-appreciated CD4+CD25+FoxP3- T cell subset that has an exhausted phenotype yet is strongly associated with favorable prognosis (see **Fig. 4**). This latter subset will be the focus of antigen discovery efforts in Task 3.

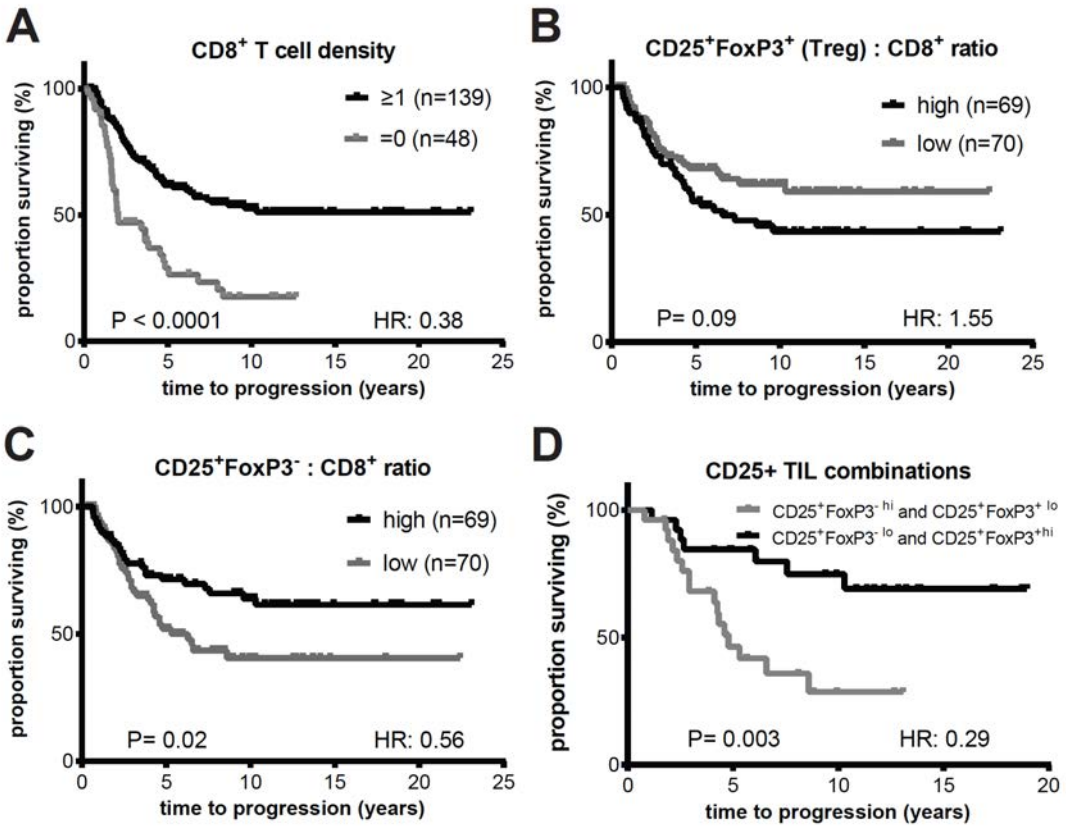

Figure 4. Prognostic significance of TIL subsets. Kaplan-Meier plots showing the association between TIL subsets and progression free-survival in a large HGSC cohort. **(A)** Density of intraepithelial CD8+ TIL. **(B)** Ratio of CD25+FoxP3+ to CD8+ TIL. **(C)** Ratio of CD25-FoxP3+ to CD8+ TIL. **(D)** Ratio of CD25+FoxP3- to CD8+ TIL. In each panel, log-rank tests were used to determine P-values, and hazard ratios (HR) are shown for each analysis. For panels B-D, analyses were restricted to cases that were positive for CD8+ TIL. Additional information can be found in deLeeuw et al. **(Appendix B)**.

Significance to the project: This data is relevant to Task 4. It confirms that CD4+CD25+FoxP3+ T cells with a classic regulatory T cell (Treg) phenotype are associated with poor prognosis. It also shows that CD4+CD25+FoxP3- T cells are strongly associated with favorable prognosis despite having an exhausted phenotype (see **Fig. 3**). This latter subset will be the focus of antigen discovery efforts in Task 3.

Published OnlineFirst December 9, 2013; DOI: 10.1158/1078-0432.CCR-13-2147

Human Cancer Biology

Clinical Cancer Research

Surveillance of the Tumor Mutanome by T Cells during Progression from Primary to Recurrent Ovarian Cancer

Darin A. Wick[1], John R. Webb[1,2], Julie S. Nielsen[1], Spencer D. Martin[1,3,4], David R. Kroeger[1], Katy Milne[1], Mauro Castellarin[3,6], Kwame Twumasi-Boateng[1], Peter H. Watson[1,2,5], Rob A. Holt[3,4,6], and Brad H. Nelson[1,2,4]

Abstract

Purpose: Cancers accumulate mutations over time, each of which brings the potential for recognition by the immune system. We evaluated T-cell recognition of the tumor mutanome in patients with ovarian cancer undergoing standard treatment.

Experimental Design: Tumor-associated T cells from 3 patients with ovarian cancer were assessed by ELISPOT for recognition of nonsynonymous mutations identified by whole exome sequencing of autologous tumor. The relative levels of mutations and responding T cells were monitored in serial tumor samples collected at primary surgery and first and second recurrence.

Results: The vast majority of mutations (78/79) were not recognized by tumor-associated T cells; however, a highly specific $CD8^+$ T-cell response to the mutation hydroxysteroid dehydrogenase–like protein 1 $(HSDL1)^{L25V}$ was detected in one patient. In the primary tumor, the $HSDL1^{L25V}$ mutation had low prevalence and expression, and a corresponding T-cell response was undetectable. At first recurrence, there was a striking increase in the abundance of the mutation and corresponding MHC class I epitope, and this was accompanied by the emergence of the $HSDL1^{L25V}$-specific $CD8^+$ T-cell response. At second recurrence, the $HSDL1^{L25V}$ mutation and epitope continued to be expressed; however, the corresponding T-cell response was no longer detectable.

Conclusion: The immune system can respond to the evolving ovarian cancer genome. However, the T-cell response detected here was rare, was transient, and ultimately failed to prevent disease progression. These findings reveal the limitations of spontaneous tumor immunity in the setting of standard treatments and suggest a high degree of ignorance of tumor mutations that could potentially be reversed by immunotherapy. *Clin Cancer Res; 20(5); 1125–34. ©2013 AACR.*

Introduction

There is long-standing interest in the concept of immune surveillance of cancer. For example, in murine models, several lines of evidence indicate that the immune system can recognize nascent tumors and prevent their outgrowth (1). In a chemical carcinogenesis model, host T cells were shown to prevent tumor development through recognition of a single somatic point mutation in the *spectrin-β2* gene (2). However, equivalent evidence of primary immune surveillance in humans is lacking, apart from T-cell–mediated control of virus-induced cancers (3). More obvious in humans is the influence of the immune system on cancer progression and clinical outcomes. In particular, the presence of $CD8^+$ tumor-infiltrating lymphocytes (TIL) is strongly associated with favorable prognosis in virtually every solid human cancer studied (4). Other TIL subsets, including $CD20^+$ B cells, further contribute to this effect (5–7). Thus, the immune system can mount seemingly protective antitumor responses in many patients with cancer.

In addition to spontaneous immune responses, there is increasing evidence that tumor immunity is enhanced by certain cancer treatments, including hormone, radiation, and chemotherapy (8). This is thought to occur by the process of immunogenic cell death, in which dying tumor cells release tumor-specific antigens and danger-associated molecules such as calreticulin, HMGB1, and ATP, leading to enhanced presentation of tumor antigens to the immune system (8). For example, we recently showed in estrogen receptor–negative breast cancer that patients with preexisting $CD8^+$ TIL show survival benefit from anthracycline-based chemotherapy, whereas patients lacking $CD8^+$ TIL do

Authors' Affiliations: [1]Trev and Joyce Deeley Research Centre, British Columbia Cancer Agency; [2]Department of Biochemistry and Microbiology, University of Victoria, Victoria; [3]Michael Smith Genome Sciences Centre, British Columbia Cancer Agency, Vancouver; Departments of [4]Medical Genetics and [5]Pathology and Laboratory Medicine, University of British Columbia, Vancouver; and [6]Department of Molecular Biology and Biochemistry, Simon Fraser University, Burnaby, British Columbia, Canada

Note: Supplementary data for this article are available at Clinical Cancer Research Online (http://clincancerres.aacrjournals.org/).

Corresponding Author: Brad H. Nelson, Trev and Joyce Deeley Research Centre, British Columbia Cancer Agency, Victoria, BC V8R 6V5, Canada. Phone: 250-519-5705; Fax: 250-519-2040; E-mail: bnelson@bccancer.bc.ca

doi: 10.1158/1078-0432.CCR-13-2147

Published OnlineFirst December 9, 2013; DOI: 10.1158/1078-0432.CCR-13-2147

Translational Relevance

Cancers progress through the accumulation of somatic mutations. To investigate how the immune system responds to the tumor genome over time, we evaluated T-cell responses to mutations identified by whole exome sequencing of serial tumor samples from 3 ovarian cancer patients undergoing standard treatment. Of 79 mutations tested, we identified a $CD8^+$ T-cell response to a point mutation in hydroxysteroid dehydrogenase–like protein 1 in one patient. This T-cell response was undetectable at diagnosis but arose during first remission in step with increased expression of the mutation. At second recurrence, the mutation continued to be expressed by tumor cells, but the T-cell response disappeared. Thus, spontaneous T-cell responses to tumor mutations are rare and transient in the context of standard treatment of ovarian cancer. The fact that many tumor mutations go unrecognized opens the possibility for immunotherapeutic targeting in the future.

not (9); this suggests that anthracyclines work in part by enhancing tumor immunity. To build on such effects, many groups are pursuing the development of immunomodulatory agents that further stimulate tumor immunity. Most notably, antibodies that block the negative regulatory molecules CTLA-4 and PD-1 on T cells have produced striking clinical responses in patients with a variety of solid tumors (10). Further enhancement of tumor immunity can potentially be achieved using therapeutic cancer vaccines or adoptive transfer of *in vitro* expanded TIL (11).

Despite the clear association between TIL and clinical outcomes, very little is known about the underlying antigens recognized by TIL. A recent study of melanoma—the best understood human cancer from an immunologic perspective—revealed that "known" antigens account for only a small percentage of TIL responses (12). This and other findings have fueled speculation that the majority of TIL might instead recognize the products of somatic mutations, collectively referred to as the "mutanome." Indeed, there have been many anecdotal reports of TIL recognizing somatic mutations in melanoma and other cancers (13). This concept received further support from a recent study in which whole exome sequencing was performed on melanoma samples from 3 patients who had responded well to therapeutic TIL infusions (14). A large proportion of T cells in the therapeutic TIL product were found to recognize MHC class I epitopes derived from 2 to 3 somatic mutations from each patient. Similar results were obtained for a patient with melanoma treated with CTLA-4 blockade (15). Thus, TIL can recognize mutant gene products, and these specificities may underlie successful immunotherapy. However, melanoma is a highly immunogenic cancer, and immunotherapy a specialized form of treatment. It is unclear whether these concepts also apply to epithelial cancers treated with conventional therapies.

High-grade serous ovarian cancer (HGSC) is a challenging disease with a 5-year survival rate of only 40% (16). A large majority of patients respond well to primary treatment with surgery and platinum- and taxane-based chemotherapy; however, most relapse within 1 to 3 years and ultimately succumb to their disease. Despite these unfortunate statistics, the presence of $CD8^+$ TIL is strongly associated with survival in HGSC, as with other cancers (17). $CD8^+$ and $CD4^+$ TIL in ovarian cancer have an activated cell surface phenotype (18, 19), show oligoclonal T-cell receptor (TCR) repertoires (20–23), and can recognize and kill autologous tumor tissue *in vitro* (22, 24–30). However, the underlying antigens remain poorly defined (24). Moreover, little is known about the fate of tumor-specific TIL as patients progress from primary to recurrent disease. A better understanding of immune activation and subsequent failure could open new frontiers in cancer immunotherapy for HGSC and other malignancies.

We recently performed whole exome sequencing of matched primary and recurrent tumor samples from 3 patients with HGSC (31). By comparing samples collected at primary surgery, first recurrence, and second recurrence, we showed that the HGSC mutanome evolves over time, likely reflecting the growth dynamics of different tumor cell subpopulations, as well as the acquisition of new mutations during chemotherapy. In this study, we investigated the hypothesis that acquired mutations might trigger responses by tumor-associated T cells, potentially resulting in immunologic selection against tumor subclones harboring such mutations.

Materials and Methods

Patients, biospecimens, and clinical data

Participant samples and clinical data were collected with informed written consent through a prospective study in partnership with the BC Cancer Agency's Tumour Tissue Repository. Ethics approval was granted by the Research Ethics Board of the BC Cancer Agency and the University of British Columbia. Patients had a diagnosis of HGSC and underwent standard treatment consisting of surgery followed by carboplatin-based chemotherapy with or without paclitaxel. Further clinical details can be found in our previous publication (31).

Malignant ascites samples were collected during primary surgery and palliative paracentesis. Ascites cells were isolated by centrifugation and crypreserved in 50% FBS, 40% complete media (RPMI 1640 containing 10% FBS, 25 mmol/L HEPES, 2 mmol/L L-glutamine, 50 μmol/L β-mercaptoethanol, and 1 mmol/L sodium pyruvate) and 10% dimethyl sulfoxide (Sigma-Aldrich). Peripheral blood mononuclear cells (PBMC) were prepared by Ficoll density centrifugation. PBMC and tumor cell preparations were stored in the vapor phase of liquid nitrogen.

Immunohistochemistry

Immunohistochemistry was performed using a Ventana Discovery XT autostainer (Ventana) with primary antibodies to CD3 (Clone SP7; Spring Biosciences, Cat. No.

Published OnlineFirst December 9, 2013; DOI: 10.1158/1078-0432.CCR-13-2147

M3074), CD8 (Clone SP16; Spring Biosciences, Cat. No. M3162), CD4 (Clone SP35; Spring Biosciences, Cat. No. M3354), CD20 (Spring Biosciences, Cat. No. E2560), MHC class I (clone EMR8-5; MBL, Cat. No. D226-3), and MHC class II (clone CR3/43, Affinity Bioreagents, Cat. No. MAI-25914). Bound antibodies were detected using a biotinylated secondary antibody (Jackson Immunoresearch) and a DABMap Kit (Ventana) followed by counterstaining with hematoxylin (Ventana). Lymphocyte densities and MHC intensity were scored by visual inspection using semiquantitative scales described in Table 1. MHC class I and class II were scored by visual inspection; the intensity of expression by tumor epithelium was scored semiquantitatively by comparison to positive stromal cells in the same or neighboring tissue cores.

In vitro T-cell line generation

Bulk ascites or tumor cells were thawed and incubated in complete media in 6-well plates at a concentration of 1×10^6 cells mL in the presence of either high-dose human interleukin (IL)-2 (6000 IU/mL; National Cancer Institute) or anti-CD3/anti-CD28–coated beads (Dynabeads Human T-Activator CD3/CD28; Life Technologies) plus low-dose IL-2 (300 IU/mL). For CD8-enriched lines, bulk ascites cells were labeled with PE-conjugated anti-human CD8 antibody (BD Biosciences), and magnetic separation was performed using anti-PE MicroBeads (Miltenyi Biotec). $CD8^+$ T cells were expanded *in vitro* using the rapid expansion protocol (REP; ref. 32). Cultures were split every 3 to 4 days with addition of fresh cytokines, and additional REPs were performed as needed. Before ELISPOT, cells were cultured in resting media consisting of complete media containing 10 ng/mL IL-7 (Peprotech) and 1 IU/mL IL-2 for 3 days.

T-cell cloning

An hydroxysteroid dehydrogenase–like protein 1 (HSDL1)-specific $CD8^+$ T-cell clone (clone 1) was generated by limiting dilution cloning. In brief, $CD8^+$ T cells from an IL-2–expanded cell line exhibiting $HSDL1^{L25V}$ reactivity were positively selected through magnetic bead separation and serially diluted down to 1 cell per well in 96-well tissue culture plates. Cultures were stimulated to proliferate by adding irradiated feeder cells (a pool of 3 irradiated allogeneic human PBMC), 30 ng/mL anti-human CD3 (eBioscience), and IL-2 (300 IU/mL). Complete media containing IL-2 was replaced every 2 to 3 days.

Table 1. Immunohistochemistry scores for TIL and MHC

	Patient 1	Patient 2	Patient 3
CD3	+++	+++	+++
CD8	++	++	+++
CD4	−	++	+
CD20	−	−	+
MHCI	+++	++	++
MHCII	+++	+	+

NOTE: TIL were scored according to the number of intraepithelial cells: +++, ≥ 20; ++, 6–19; +, 1–5; or −, 0. MHC expression by tumor epithelium was scored semiquantitatively by comparison to positive stromal cells in the same or neighboring tissue cores: +++, strong; ++, moderate; +, weak; −, negative.

Flow cytometry

Bulk ascites cells were assessed directly *ex vivo* by staining with antibodies to CD4 or CD8 in combination with an anti-TCR Vβ repertoire panel (IOTEST BetaMark; Beckman Coulter) and analyzed with a Becton Dickinson FACSCalibur.

Epitope prediction and peptide design

Whole exome sequencing results were previously published (31). HLA typing was performed as previously described (33) and analyzed using IMGT/HLA database version 3.3.0. Peptide/MHC binding scores for all possible 8-, 9-, 10-, and 11-amino acid in length peptides containing the mutated residue relative to each patient's MHC class I alleles were generated using the epitope prediction software NetMHCpan-2.4 (ref. 34; Supplementary Tables S1–S4). All peptides predicted to bind MHC with an affinity ≤50 nmol/L were selected for screening. In addition, for those mutations that did not yield peptides with binding scores of ≤50 nmol/L, the minimal peptide with the highest predicted MHC binding affinity was selected. In addition to predicted minimal peptides, for each mutation, we designed 3 overlapping 15-mer peptides with a 12-residue overlap such that all possible 8-, 9-, 10-, and 11-mer peptides containing the point mutation were represented, as well as many MHC class II binding peptides. Initial screens used crude peptides, whereas all subsequent experiments involving HSDL1 used peptides with >90% purity. Peptides were commercially synthesized (Genscript) and reconstituted in dimethyl sulfoxide (Sigma-Aldrich).

IFN-γ ELISPOT

Standard IFN-γ ELISPOT assays were performed as previously described (35). Predicted minimal peptides and overlapping 15-mer peptides were added to wells at a final concentration of 10 μg/mL. Wells containing anti-CD3/anti-CD28 coated beads (bead-to-cell ratio of 1:1) or human cytomegalovirus, Epstein-Barr virus, and influenza virus (CEF) peptides (10 μg/mL; Anaspec) served as positive controls. Spots were enumerated using an automated plate reader (AID GmbH). We defined responses using empirical response methods: positive wells were required to contain a minimum of 10 spots/2×10^5 cells and have at least 3-fold more spots than negative control wells. These criteria have been shown to yield very low false positive rates (36).

To determine HLA restriction of the HSDL1 reactive clone from patient 3, B-lymphoblastoid cell lines (B-LCL) matched at 0 to 3 HLA alleles and corresponding to all 6 HLA class I alleles from patient 3 were obtained from an

Published OnlineFirst December 9, 2013; DOI: 10.1158/1078-0432.CCR-13-2147

in-house B-LCL bank or the Fred Hutchinson Cancer Research Center International Histocompatibility Working Group Cell and Gene Bank (Seattle, WA). HLA restriction was determined by IFN-γ ELISPOT using 9,000 cells/well of clone 1 incubated with 2×10^5 B-LCL pulsed with the CYMEAVAL minimal peptide (10 μg/mL).

Clone 1 (10^5 cells/well) was assessed by IFN-γ ELISPOT for recognition of ascites tumor samples (10^5 cells/well), which had been depleted of $CD45^+$ cells by magnetic bead separation (Miltenyi Biotec). An autologous $CD4^+$ T-cell line served as a negative control target. CD45- ascites and the $CD4^+$ T-cell line were pulsed with CYMEAVAL peptide (10 μg/mL for 2 hours) and used as a positive control.

PCRs

To measure the relative abundance of the clone 1 TCR-β transcript, RNA from ascites samples and IL-2 expanded T-cell lines was isolated using the AllPrep DNA/RNA Isolation Kit (Qiagen) and converted to cDNA using a qScript cDNA Synthesis Kit (Quanta Biosciences). A TRVB6-6-specific forward primer (TCACTGATAAAGGAGAAGTCCCG) and CDR3 clone-specific primer (AGTACTGGGTCTCTACGGCC) were used to amplify a 150 bp region of the TCR-β of clone 1. Actin transcript was amplified as a reference (forward primer CGTCTTCCCCTCCATCGTG; reverse primer TTCTCCATGTCGTCCCAGTTG). Amplification of target genes was detected using perfeCTa green supermix (Quanta Biosciences) and analyzed with a MyiQ thermocycler (Bio-Rad). By serial dilution of clone 1 into irrelevant polyclonal $CD8^+$ T cells, the sensitivity of detection was determined to be approximately $1{:}10^5$ T cells.

Results

Patient characteristics and mutational profiles

All 3 HGSC cases showed evidence of spontaneous tumor immunity as indicated by the presence of intraepithelial TIL expressing CD3, CD8, and in some cases CD4 and CD20 (Table 1 and Supplementary Fig. S1). Moreover, tumors from all 3 patients expressed MHC class I and variable levels of MHC class II. Patients underwent standard treatment consisting of cytoreductive surgery followed by platinum-based chemotherapy with or without taxanes (Fig. 1). Patients 1 and 2 showed partial responses to primary treatment, whereas patient 3 achieved an initial clinical remission. All patients experienced progressive or recurrent disease, at which time they received additional chemotherapy. Patients 1 and 2 were generally nonresponsive to second line treatment, whereas patient 3 again achieved clinical remission, albeit for a shorter interval than the first remission. All 3 patients received a third cycle of chemotherapy, after which they succumbed to their disease. Additional clinical details have been published (31).

As previously reported, we performed whole exome sequencing on ascites tumor samples from these 3 patients (31). Recognizing the considerable spatial and temporal heterogeneity of mutational profiles in prior studies of HGSC (31, 37, 38), we elected to sequence tumor cells from the ascites compartment rather than solid tumor,

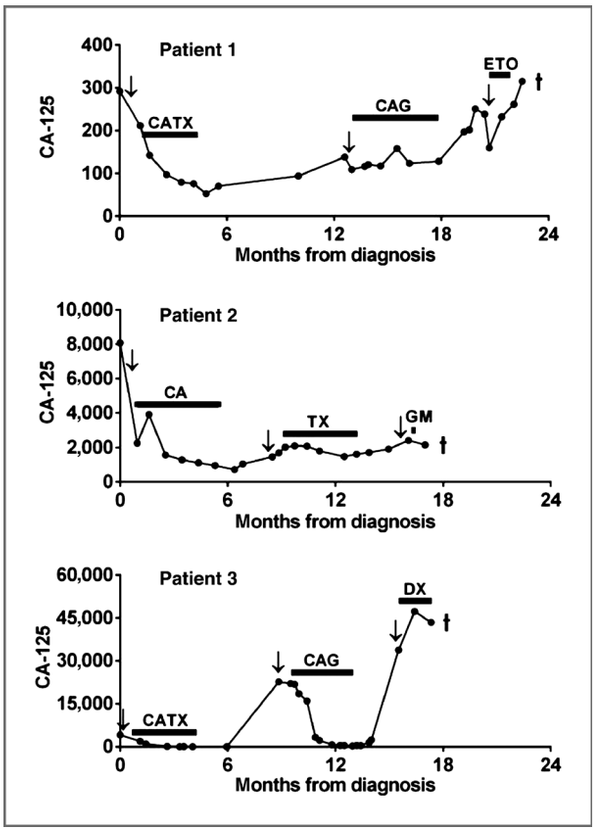

Figure 1. Clinical course of the 3 study patients. All 3 patients were diagnosed with HGSC and underwent cytoreductive surgery at $t = 0$. Tumor burden is indicated by blood CA-125 levels (U/mL; black dots). Chemotherapy cycles are indicated by horizontal black bars and involved the following drugs: CATX, carboplatin with paclitaxel; CAG, carboplatin with gemcitabine; ETO, etoposide; CA, carboplatin; TX, taxol; GM, gemcitabine; DX, pegylated liposomal doxorubicin. Downward arrows indicate time points at which ascites samples (containing tumor cells and TAL) were collected. The cross symbol indicates the time of death. These and additional clinical data have been previously published (31).

reasoning that ascites would contain cells from multiple tumor regions. To address temporal heterogeneity, we sequenced tumor cells from 3 clinical time points, including primary surgery, first recurrence, and second recurrence. Patients 1 and 2 had a total of 22 and 31 mutations, respectively, and their mutational profiles were relatively stable, with only 1 and 6 mutations appearing or disappearing during disease progression. Patient 3 had a total of 40 mutations and a less stable mutational profile, with 11 mutations appearing or disappearing over time. Additional details about mutational profiles have been published (31).

Screening for T-cell responses to tumor mutations

We investigated whether the 3 patients had spontaneous T-cell responses to the mutations identified by whole exome sequencing. Given that the mutational profiles were derived from ascites tumor samples, we assessed tumor-associated lymphocyte (TAL) lines derived from matched ascites samples. In initial experiments, TAL were expanded using

Published OnlineFirst December 9, 2013; DOI: 10.1158/1078-0432.CCR-13-2147

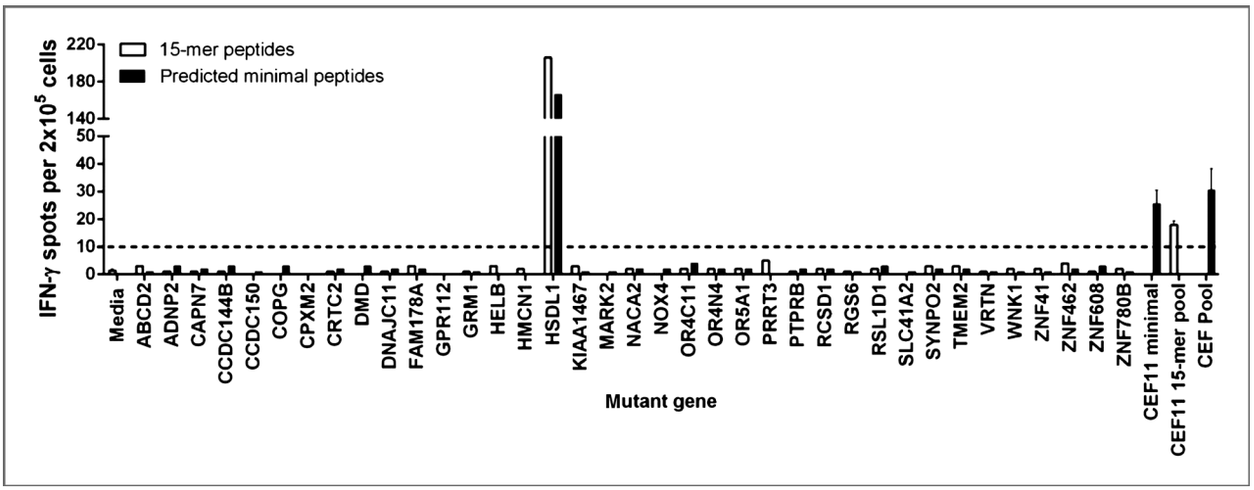

Figure 2. T-cell responses to tumor-specific mutations in HGSC. A, T-cell line was derived from the first recurrence ascites sample of patient 3 using high-dose IL-2 and assessed by IFN-γ ELISPOT for recognition of peptides encoding 37 mutations. For each mutation, the T-cell line was exposed to the predicted minimal peptides (black bars) and a set of 3 overlapping 15-mer peptides (white bars). Robust responses were seen against both the predicted minimal peptides and overlapping 15-mers encoding the HSDL1^{L25V} mutation. As positive controls, cells were stimulated with a pool of minimal CEF peptides, as well as minimal and overlapping 15-mers corresponding to a single HLA-A2–restricted CEF epitope (CEF11). Responses are shown as the number of IFN-γ spot-forming cells per 2×10^5 total lymphocytes in expanded cultures. The hashed line represents the threshold for positivity (3 times background). Data are shown as the mean ± SD from 1 of 2 independent experiments.

a well-established method involving high-dose IL-2 (32). TAL lines were tested by IFN-γ ELISPOT for recognition of (a) predicted minimal peptides (Supplementary Tables S1–S3) and (b) overlapping 15-mer peptides corresponding to all of the mutations found in the respective patient's tumor samples. This dual strategy captured the benefits of epitope prediction while additionally providing unbiased coverage of all possible MHC class I epitopes and many class II epitopes (39). We tested all identified nonsynonymous mutations except those that were present in germline (e.g., BRCA1), or resulted in nontranslated genes (e.g., SPATS2^{MIV}), or resulted in premature stop codons. Moreover, mutations were tested irrespective of their expression level to avoid excluding mutant gene products that might have been downregulated as a result of immune selection.

For patients 1 and 2, the IL-2–expanded TAL lines failed to respond to any of the mutant peptides at any of the time points (Supplementary Fig. S2). As positive controls, TAL lines responded to peptides from common viral antigens (CEF peptides) to which the patients had previously been found to respond. As an additional positive control, TAL lines responded strongly to stimulation with anti-CD3/anti-CD28 coated beads (data not shown). To mitigate the concern that mutation-specific T cells might have been lost during IL-2 expansion, we generated additional T-cell lines from ascites samples using an alternate expansion method involving anti-CD3/anti-CD28 coated beads. In addition, we tested TAL directly *ex vivo* in bulk ascites samples. As before, we failed to detect T-cell responses to any of the mutant peptides, whereas T-cell responses were seen to the CEF peptides and anti-CD3/anti-CD28–coated beads (data not shown).

In contrast to the first 2 patients, TAL lines from patient 3 showed a clear response to predicted minimal and 15-mer peptides corresponding to a point mutation in the hydroxysteroid dehydrogenase-like protein 1 gene (HSDL1^{L25V}; Fig. 2). This T-cell response was detected in TAL lines generated with high-dose IL-2 (Fig. 2) or anti-CD3/anti-CD28 beads, but it was not detected directly *ex vivo* in bulk ascites samples (data not shown). Moreover, the T-cell response was only detected in TAL lines from the first recurrence sample. We failed to see T-cell responses to peptides corresponding to any of the other mutations from patient 3, despite clear responses to the positive controls (Fig. 2 and data not shown). No mutation-specific responses were detected using anti-CD3/anti-CD28–expanded T cells from the primary solid tumor (data not shown). Thus, we focused our analysis on the T-cell response to HSDL1^{L25V}.

Characterizing the T-cell response to HSDL1^{L25V}

By assessing magnetically sorted CD4$^+$ and CD8$^+$ T-cell populations, we determined that the response to HSDL1^{L25V} was mediated exclusively by CD8$^+$ T cells (data not shown). A CD8$^+$ T-cell clone recognizing HSDL1^{L25V} (clone 1) was generated by limiting dilution cloning of CD8$^+$ T cells from an IL-2–expanded TAL line. The TCR from clone 1 was amplified by PCR and sequenced, which revealed a single TCR-β sequence and both a productive and nonproductive TCR-α gene (data not shown). When clone 1 was tested by IFN-γ ELISPOT against a panel of all 8-, 9-, 10-, and 11-mer peptides spanning the HSDL1^{L25V} point mutation, the 8 amino acid sequence CYMEAVAL was defined as the minimal epitope (Supplementary Fig. S3). Using a panel of partially HLA-matched allogeneic B cell lines, we determined that clone 1 recognized CYMEAVAL in the context of HLA-C*14:03 (Supplementary Fig. S4). This interaction was also predicted by the NetMHCpan-2.4

Published OnlineFirst December 9, 2013; DOI: 10.1158/1078-0432.CCR-13-2147

algorithm in that CYMEAVAL had the strongest predicted HLA binding score of all candidate epitopes encoding HSDL1^{L25V} across all 6 HLA alleles for this patient (Supplementary Table S3). Notably, clone 1 demonstrated absolute specificity for mutated HSDL1 when assessed using either minimal peptides or 15-mer peptides comprising the wild-type HSDL1 sequence (Fig. 3).

Recognition of autologous tumor by the HSDL1^{L25V}-specific CD8$^{\pm}$ T-cell clone

Based on read counts from the whole exome sequencing data, the relative frequency of the HSDL1^{L25V} allele increased from 3.5% in the primary sample to 55.0% and 60.2% in the first and second recurrent samples (Fig. 4A; ref. 31). Thus, there was an increase in the number of cells harboring the HSDL1^{L25V} point mutation during the progression from primary to recurrent disease. To assess the corresponding expression and presentation of the CYMEAVAL epitope over time, clone 1 was tested by IFN-γ ELISPOT for recognition of serial tumor samples. Clone 1 responded to tumor samples from all 3 time points (Fig. 4B). However, the 2 recurrent tumor samples elicited a far stronger response than the primary tumor sample. In contrast, all 3 tumor samples elicited strong responses from clone 1 when pulsed with CYMEAVAL peptide, indicating they were all conducive to T-cell stimulation when the epitope was not limiting (data not shown). Thus, it seems that the abundance of the CYMEAVAL epitope increased significantly between the time of primary surgery and first recurrence and was maintained at second recurrence.

We next examined the activity and abundance of HSDL1^{L25V}-specific T cells in tumor samples from the 3 time points. By IFN-γ ELISPOT, HSDL1^{L25V}-specific T-cell responses were only seen with *in vitro* expanded TAL lines derived from the first recurrence (Fig. 4C). To further investigate whether HSDL1^{L25V}-specific T cells might be present at the other 2 time points, we performed additional TAL expansions. Knowing that clone 1 was CD8^{+}, we used magnetic beads to enrich CD8^{+} T cells from *ex vivo* ascites and then expanded them using a REP (32). Despite using highly purified CD8^{+} lines, we again only detected an HSDL1^{L25V}-specific T-cell response in the line derived from the first recurrence (data not shown). Intriguingly, this response was greatly diminished compared with that previously seen with the high-dose IL-2–derived TAL line, indicating that clone 1 expanded preferentially under the high-dose IL-2 condition. In summary, using several expansion methods, HSDL1^{L25V}-specific T cells were only detected at first recurrence, despite the fact that the HSDL1^{L25V} gene and CYMEAVAL epitope were abundant at both first and second recurrences.

To quantify HSDL1^{L25V}-specific T cells independent of their ability to make IFN-γ, we considered measuring their abundance directly with an MHC class I tetramer. However, tetramer reagents for HLA-C*14:03 are not currently available. Moreover, flow cytometry with an antibody to the Vβ region used by clone 1 (Vβ 13.6) indicated that clone 1 represented at most 0.5% of CD8^{+} TAL at any time point (Supplementary Fig. S4A), indicating that there would be insufficient events for robust analysis with the available biospecimens. Instead, we designed clonotype-specific primers and measured TCR-β chain levels by quantitative PCR of genomic DNA and cDNA. By titrating known numbers of clone 1 T cells into a polyclonal CD8^{+} T-cell preparation, we found that the limit of detection of the PCR assay was approximately 1:10^{5} cells (data not shown). By this assay, the presence of clone 1 paralleled that seen by ELISPOT in that (i) clone 1 was not detected directly *ex vivo* (i.e., in nonexpanded ascites samples), and (ii) it was detected in IL-2- or anti-CD3/anti-CD28 bead-expanded TAL lines from the first recurrence but not the primary sample or second recurrence (Fig. 4D). The PCR assay further revealed that clone 1 was not detectable in primary solid tumor. Thus, it seems that clone 1 arose during the first remission in step with the increasing abundance of the HSDL1^{L25V} epitope but disappeared during the second remission despite continued expression of the epitope.

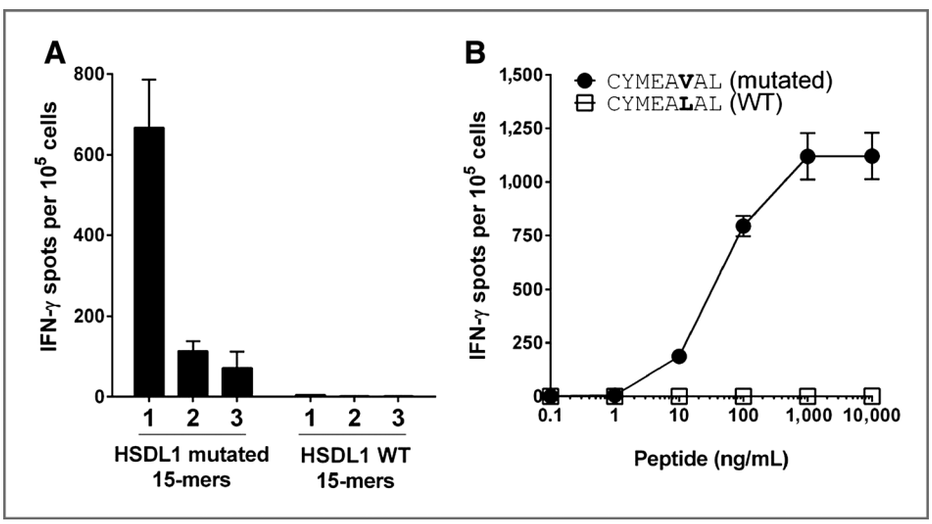

Figure 3. Clone 1 shows absolute specificity for mutated HSDL1. An HSDL1^{L25V}-specific CD8^{+} T-cell clone (clone 1) was assessed by IFN-γ ELISPOT for responses to (A) overlapping mutated and wild-type 15-mer peptides spanning the L25V point mutation (1 = HSDL1$_{15\text{-}29}$, 2 = HSDL1$_{18\text{-}32}$, 3 = HSDL1$_{21\text{-}35}$), or (B) a titration of minimal peptides encoding mutated (CYMEAVAL, closed circles) or wild-type (CYMEALAL, open squares) HSDL1. Responses are shown as the mean ± SD of IFN-γ spot-forming cells per 1 × 10^{5} total cells.

Published OnlineFirst December 9, 2013; DOI: 10.1158/1078-0432.CCR-13-2147

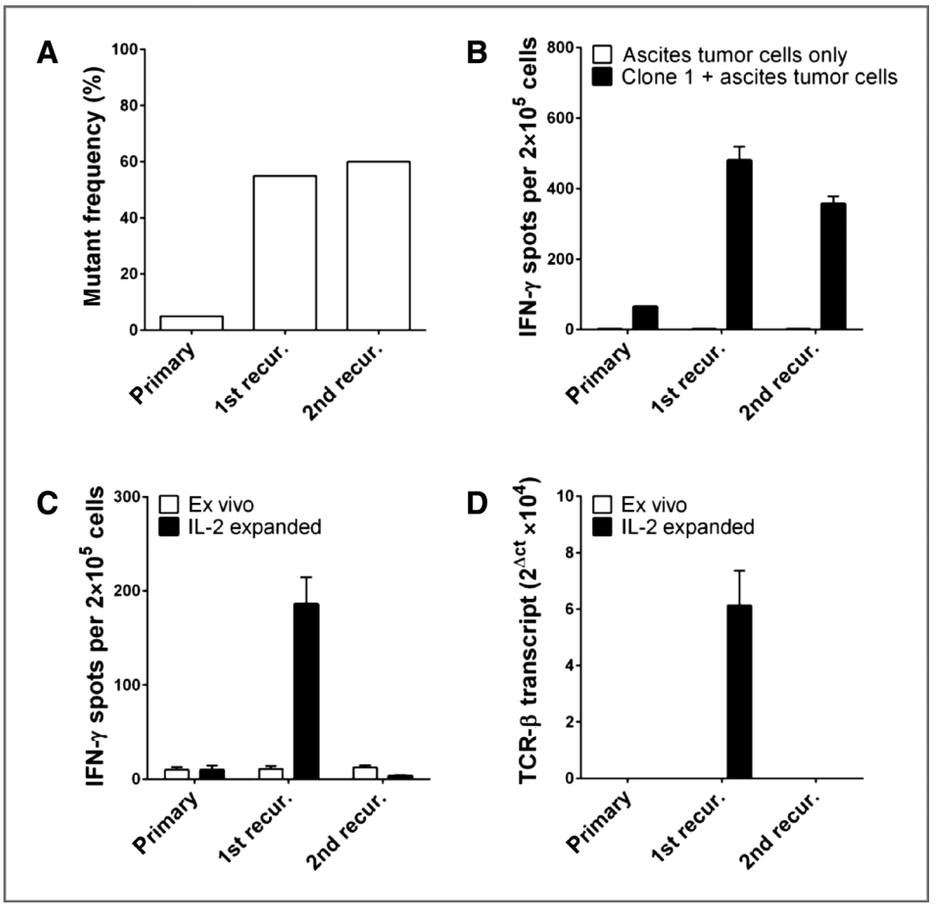

Figure 4. Dynamics of the HSDL1^{L25V} mutation and corresponding CD8$^+$ T-cell response during disease progression. A, to assess the abundance and expression of HSDL1^{L25V} in tumor samples over time, the allelic frequencies of mutant versus wild-type HSDL1 genes were inferred from whole exome sequencing data of CD45-depleted tumor samples [80%–99% CD45$^-$ by flow cytometry (31)]. B, to determine whether the HSDL1^{L25V} epitope was presented by tumor cells, clone 1 was assessed by IFN-γ ELISPOT for recognition of autologous CD45-depleted ascites tumor samples (96%–98% CD45$^-$ by flow cytometry) from primary and recurrent time points. An autologous CD4$^+$ T-cell line served as a negative control in place of tumor cells. Responses are shown as the number of IFN-γ spot-forming cells per 2×10^5 total cells as measured by IFN-γ ELISPOT assay. C, to measure the magnitude of the CD8$^+$ T-cell response to HSDL1^{L25V} over time, cells from the ascites at each time point were assessed directly *ex vivo* (white bars) and after expansion with high-dose IL-2 (black bars) for responses to the minimal epitope (CYMEAVAL) by IFN-γ ELISPOT. Responses are shown as the number of IFN-γ spot-forming cells per 2×10^5 total cells. Similar results were obtained using overlapping 15-mer peptides (data not shown). D, to directly measure the abundance of clone 1 in tumor samples, the corresponding clonotype-specific TCR-β sequence was detected by quantitative PCR of cDNA from *ex vivo* ascites samples and IL-2-expanded T-cell lines (from C). Data are shown as the mean ± SD.

Discussion

We systematically assessed the extent to which the mutant genome is recognized by the immune system in the context of standard treatment of HGSC. By studying a panel of 79 mutations from 3 patients and 3 clinical time points, we found a CD8$^+$ T-cell response to the point mutation HSDL1^{L25V} in 1 patient. This response was undetectable in the primary ascites and solid tumor samples, but emerged by the time of first recurrence, alongside a marked increase in expression of the mutant epitope by tumor cells. The patient underwent additional chemotherapy and achieved a second remission period, but this was short lived. At second recurrence, the mutant epitope was still abundant in tumor tissue, but the mutation-specific T-cell response was no longer detectable. Thus, it seems that during the first remission period, the immune system of this patient mounted a T-cell response against a mutation expressed by an expanding tumor subclone, but this response ultimately faltered. Our results provide an example of the unaided immune system responding to the changing tumor mutanome, yet ultimately failing to eliminate mutation-bearing tumor cells. The rare, weak, and transient nature of the response described here highlights the general inadequacy of immune surveillance in the context of standard treatment, which is consistent with the high mortality rate for HGSC. On the positive side, our results leave open the possibility that the mutanome might represent an untapped reservoir of target antigens for immunotherapy.

A key finding of this study is that only a small proportion of tumor mutations (1/79 or 1.3% across 3 patients) seem to be spontaneously recognized by autologous T cells. Our conclusion is based on a comprehensive screening method

Published OnlineFirst December 9, 2013; DOI: 10.1158/1078-0432.CCR-13-2147

that utilized predicted high-affinity peptides as well as unbiased overlapping 15-mer peptides. In theory, this method should be able to detect responses to all MHC class I epitopes, as well as many MHC class II epitope containing the mutation. Moreover, we interrogated TAL samples from 3 clinical time points, both directly *ex vivo* and after *in vitro* expansion by multiple methods so as to circumvent any immunosuppressive effects of the tumor environment. A low percentage of immunogenic mutations was also recently reported in advanced melanoma. Robbins and colleagues used whole exome sequencing to identify mutations in tumor samples from 3 patients, each of whom had shown an objective response to autologous TIL therapy (14). They identified 264 to 574 nonsynonymous mutations per tumor, of which 2 to 3 mutations per patient were specifically recognized by $CD8^+$ T cells from the therapeutic TIL product. Thus, this study too found responses to only 0.3% to 1.1% of mutations, despite selecting patients who had responded well to TIL therapy and hence had demonstrably immunogenic tumors. Similarly, using an HLA tetramer-based assay, Schumacher and colleagues recently reported that only 2 of 448 predicted mutant $CD8^+$ T-cell epitopes were recognized by $CD8^+$ TIL from a patient with melanoma (15). Although additional studies are required, these data combined with ours indicate that only a minor fraction of point mutations spontaneously trigger T-cell responses. However, it remains possible that other types of mutations such as amplifications, gene fusions, or other large structural rearrangements might prove more immunogenic.

The above conclusion leads to the question of why the remaining 99% of mutations did not trigger a detectable T-cell response in patients. It is possible that additional T-cell responses could have been detected by measuring other markers of T-cell activation or using other assay methods, although IFN-γ ELISPOT is widely used as an indicator of tumor reactivity (40). Apart from detection methods, mutated gene products can be invisible to T cells for elementary reasons such as insufficient expression, lack of a high affinity MHC class I or II epitope, or absence of a corresponding TCR in the patient's T-cell repertoire. In contrast, mutations that give rise to bona fide epitopes for which a corresponding T cell is present are potentially visible to the immune system. Yet responses to such mutations might still be thwarted by factors such as peripheral tolerance or immune suppression (41). Another possibility is immunologic ignorance, in which a potentially visible mutation fails to elicit a T-cell response because of ineffective priming, competition from higher affinity peptides, physical barriers, or other mechanisms (42, 43). We do not know how many of the mutations studied here were subject to immunologic ignorance, as our stimulation methods were not designed to prime naïve T-cell responses. However, such mutations are worthy of further study, as they represent an attractive class of potential target antigens for immunotherapy (44).

Although our sample size was small, we considered several possible reasons why patient 3 mounted a mutation-specific T-cell response whereas the other 2 patients did not. First, patient 3 had more mutations than the other patients, which increases the mathematical probability of having an immunogenic mutation. Second, patient 3 showed the greatest number of changes in the mutanome over time (11 changes vs. 1–6 changes). Indeed, the prevalence of the $HSDL1^{L25V}$ mutation increased from 3.5% to 60% of sequencing reads during progression from primary to recurrent disease; the corresponding increase in the abundance of the mutant epitope might have been sufficient to break immunologic ignorance or tolerance. Third, patient 3 experienced the greatest decrease in tumor burden during chemotherapy (Fig. 1; ref. 31). There is increasing evidence that chemotherapy can induce tumor immunity by causing the release of tumor antigens as well as signaling molecules such as HMGB1, ATP, and calreticulin (8). Reduced tumor burden can also provide relief from tumor-associated immunosuppressive factors. Further work with additional patients will be required to better define the factors that induce spontaneous antitumor immune responses during standard treatments.

Despite being present at first recurrence, clone 1 failed to prevent the outgrowth of antigen-positive tumor at second recurrence, suggesting that a profound impairment of this response occurred. A wide variety of immune suppressive mechanisms could have contributed to this phenomenon, including regulatory T cells, myeloid-derived suppressor cells, indoleamine 2,3-dioxygenase, and PD-L1, each of which has been reported in ovarian cancer and can impair T-cell expansion and function (45–47). In addition, the fact that a large proportion of tumor cells continued to present the mutant epitope at second recurrence suggests that clone 1 may have experienced chronic antigen exposure. This can lead to loss of T-cell functions in a defined sequence: IL-2 production → cytolytic activity → proliferation → IFN-γ → apoptosis (clonal deletion; ref. 48). With IFN-γ ELISPOT, one can detect T cells even at the far end of this continuum, underscoring the appropriateness of this assay. However, at second recurrence, clone 1 was undetectable not only by ELISPOT but also by PCR, which would be consistent with clonal deletion. This raises the specter that other tumor-specific T-cell responses might have experienced a similar fate earlier in tumor progression, contributing to the negative results for other mutations.

Looking forward, our results raise the possibility of targeting the potentially large reservoir of mutant epitopes that are visible to the immune system yet go unrecognized. This might be achieved with immune modulating strategies such as CTLA-4 or PD-1 blockade (10). Notably, a large proportion of $CD8^+$ TAL in patient 3 expressed PD-1 by flow cytometry (data not shown), suggesting their activity could potentially have been enhanced by PD-1 blockade. Looking ahead to an era in which mutanome data are available for most patients with cancer, one can envision using mutation-encoding vaccines to focus T-cell responses more specifically toward tumor cells, as recently demonstrated in a mouse model of melanoma (49). Indeed, one can speculate that vaccination against the $HSDL1^{L25V}$ mutation during first remission might have prevented the expansion of the

Published OnlineFirst December 9, 2013; DOI: 10.1158/1078-0432.CCR-13-2147

corresponding tumor subclone in patient 3. However, this example also raises the important issue of intratumoral heterogeneity, as the HSDL1^{L25V} mutation at its peak was present in only 60% of sequencing reads, suggesting it may not have been present in all tumor cells. Tumor heterogeneity can potentially be addressed by targeting multiple mutations that collectively cover the complete phylogeny of tumor subclones. Alternatively, one could attempt to target mutations that arise early in tumorigenesis and are present in all tumor cells. A recent study of spatial heterogeneity in HGSC revealed that tumors harbor 15 to 55 such mutations (37). In summary, our findings with the HSDL1^{L25V} mutation illustrate the importance of developing immunotherapeutic strategies that not only overcome immune suppression but also contend with the spatial and temporal heterogeneity of the tumor genome.

Disclosure of Potential Conflicts of Interest

No potential conflicts of interest were disclosed.

Authors' Contributions

Conception and design: D.A. Wick, J.R. Webb, J.S. Nielsen, S.D. Martin, R.A. Holt, B.H. Nelson

Development of methodology: D.A. Wick, J.R. Webb, J.S. Nielsen, S.D. Martin, K. Milne, M. Castellarin, R.A. Holt, B.H. Nelson

Acquisition of data (provided animals, acquired and managed patients, provided facilities, etc.): D.A. Wick, J.R. Webb, J.S. Nielsen, D.R. Kroeger, K. Milne, K. Twumasi-Boateng

Analysis and interpretation of data (e.g., statistical analysis, biostatistics, computational analysis): D.A. Wick, J.R. Webb, J.S. Nielsen, S.D. Martin, D.R. Kroeger, M. Castellarin, P.H. Watson, B.H. Nelson

Writing, review, and/or revision of the manuscript: D.A. Wick, J.R. Webb, J.S. Nielsen, S.D. Martin, D.R. Kroeger, K. Milne, M. Castellarin, P. H. Watson, R.A. Holt, B.H. Nelson

Administrative, technical, or material support (i.e., reporting or organizing data, constructing databases): K. Milne, B.H. Nelson

Study supervision: R.A. Holt, B.H. Nelson

Acknowledgments

The authors thank the study participants for donating biospecimens and clinical data; Dr. E. McMurtrie for patient referrals; and J. LeBlanc, S. Babinsky, and K. Dillon for technical assistance.

Grant Support

This study was supported by the U.S. Department of Defense, Genome British Columbia, BC Cancer Agency Tumour Tissue Repository (a member of the Canadian Tumor Repository Network), and the British Columbia Cancer Foundation.

The costs of publication of this article were defrayed in part by the payment of page charges. This article must therefore be hereby marked advertisement in accordance with 18 U.S.C. Section 1734 solely to indicate this fact.

Received August 6, 2013; revised October 29, 2013; accepted December 5, 2013; published OnlineFirst December 9, 2013.

References

1. Schreiber RD, Old LJ, Smyth MJ. Cancer immunoediting: integrating immunity's roles in cancer suppression and promotion. Science 2011;331:1565–70.
2. Matsushita H, Vesely MD, Koboldt DC, Rickert CG, Uppaluri R, Magrini VJ, et al. Cancer exome analysis reveals a T-cell-dependent mechanism of cancer immunoediting. Nature 2012;482:400–4.
3. Martin D, Gutkind JS. Human tumor-associated viruses and new insights into the molecular mechanisms of cancer. Oncogene 2008; 27:S31–42.
4. Fridman WH, Pages F, Sautes-Fridman C, Galon J. The immune contexture in human tumours: impact on clinical outcome. Nat Rev Cancer 2012;12:298–306.
5. Nielsen JS, Sahota RA, Milne K, Kost SE, Nesslinger NJ, Watson PH, et al. CD20+ tumor-infiltrating lymphocytes have an atypical CD27− memory phenotype and together with CD8+ T cells promote favorable prognosis in ovarian cancer. Clin Cancer Res 2012; 18:3281–92.
6. Milne K, Kobel M, Kalloger SE, Barnes RO, Gao D, Gilks CB, et al. Systematic analysis of immune infiltrates in high-grade serous ovarian cancer reveals CD20, FoxP3 and TIA-1 as positive prognostic factors. PLoS ONE 2009;4:e6412.
7. Nelson BH. CD20+ B cells: the other tumor-infiltrating lymphocytes. J Immunol 2010;185:4977–82.
8. Kroemer G, Galluzzi L, Kepp O, Zitvogel L. Immunogenic cell death in cancer therapy. Annu Rev Immunol 2013;31:51–72.
9. West NR, Milne K, Truong PT, Macpherson N, Nelson BH, Watson PH. Tumor-infiltrating lymphocytes predict response to anthracycline-based chemotherapy in estrogen receptor-negative breast cancer. Breast Cancer Res 2011;13:R126.
10. Postow MA, Harding J, Wolchok JD. Targeting immune checkpoints: releasing the restraints on anti-tumor immunity for patients with melanoma. Cancer J 2012;18:153–9.
11. Mellman I, Coukos G, Dranoff G. Cancer immunotherapy comes of age. Nature 2011;480:480–9.
12. Andersen RS, Thrue CA, Junker N, Lyngaa R, Donia M, Ellebaek E, et al. Dissection of T-cell antigen specificity in human melanoma. Cancer Res 2012;72:1642–50.
13. Sensi M, Anichini A. Unique tumor antigens: evidence for immune control of genome integrity and immunogenic targets for T cell-mediated patient-specific immunotherapy. Clin Cancer Res 2006; 12:5023–32.
14. Robbins PF, Lu YC, El-Gamil M, Li YF, Gross C, Gartner J, et al. Mining exomic sequencing data to identify mutated antigens recognized by adoptively transferred tumor-reactive T cells. Nat Med 2013;19: 747–52.
15. van Rooij N, van Buuren MM, Philips D, Velds A, Toebes M, Heemskerk B, et al. Tumor exome analysis reveals neoantigen-specific T-cell reactivity in an ipilimumab-responsive melanoma. J Clin Oncol 2013;31:doi: 10.1200/JCO.2012.47.7521.
16. Vaughan S, Coward JI, Bast RCJr, Berchuck A, Berek JS, Brenton JD, et al. Rethinking ovarian cancer: recommendations for improving outcomes. Nat Rev Cancer 2011;11:719–25.
17. Hwang WT, Adams SF, Tahirovic E, Hagemann IS, Coukos G. Prognostic significance of tumor-infiltrating T cells in ovarian cancer: a meta-analysis. Gynecol Oncol 2012;124:192–8.
18. Santin AD, Hermonat PL, Ravaggi A, Bellone S, Roman JJ, Smith CV, et al. Phenotypic and functional analysis of tumor-infiltrating lymphocytes compared with tumor-associated lymphocytes from ascitic fluid and peripheral blood lymphocytes in patients with advanced ovarian cancer. Gynecol Obstet Invest 2001;51:254–61.
19. Melichar B, Nash MA, Lenzi R, Platsoucas CD, Freedman RS. Expression of costimulatory molecules CD80 and CD86 and their receptors CD28, CTLA-4 on malignant ascites CD3+ tumour-infiltrating lymphocytes (TIL) from patients with ovarian and other types of peritoneal carcinomatosis. Clin Exp Immunol 2000;119: 19–27.
20. Pappas J, Jung WJ, Barda AK, Lin WL, Fincke JE, Purev E, et al. Substantial proportions of identical beta-chain T-cell receptor transcripts are present in epithelial ovarian carcinoma tumors. Cell Immunol 2005;234:81–101.
21. Halapi E, Yamamoto Y, Juhlin C, Jeddi-Tehrani M, Grunewald J, Andersson R, et al. Restricted T cell receptor V-β and J-β usage in T cells from interleukin-2-cultured lymphocytes of ovarian and renal carcinomas. Cancer Immunol Immunother 1993;36:191–7.

Published OnlineFirst December 9, 2013; DOI: 10.1158/1078-0432.CCR-13-2147

22. Peoples GE, Davey MP, Goedegebuure PS, Schoof DD, Eberlein TJ. T cell receptor V β 2 and V β 6 mediate tumor-specific cytotoxicity by tumor-infiltrating lymphocytes in ovarian cancer. J Immunol 1993; 151:5472–80.
23. Peoples GE, Yoshino I, Douville CC, Andrews JV, Goedegebuure PS, Eberlein TJ. TCR V β 3+ and V β 6+ CTL recognize tumor-associated antigens related to HER2/neu expression in HLA-A2+ ovarian cancers. J Immunol 1994;152:4993–9.
24. Nelson BH. The impact of T-cell immunity on ovarian cancer outcomes. Immunol Rev 2008;222:101–16.
25. Goedegebuure PS, Douville CC, Doherty JM, Linehan DC, Lee KY, Ganguly EK, et al. Simultaneous production of T helper-1-like cytokines and cytolytic activity by tumor-specific T cells in ovarian and breast cancer. Cell Immunol 1997;175:150–6.
26. Ioannides CG, Freedman RS, Platsoucas CD, Rashed S, Kim YP. Cytotoxic T cell clones isolated from ovarian tumor-infiltrating lymphocytes recognize multiple antigenic epitopes on autologous tumor cells. J Immunol 1991;146:1700–7.
27. Ioannides CG, Platsoucas CD, Rashed S, Wharton JT, Edwards CL, Freedman RS. Tumor cytolysis by lymphocytes infiltrating ovarian malignant ascites. Cancer Res 1991;51:4257–65.
28. Dadmarz RD, Ordoubadi A, Mixon A, Thompson CO, Barracchini KC, Hijazi YM, et al. Tumor-infiltrating lymphocytes from human ovarian cancer patients recognize autologous tumor in an MHC class II-restricted fashion. Cancer J Sci Am 1996;2:263–72.
29. Peoples GE, Schoof DD, Andrews JV, Goedegebuure PS, Eberlein TJ. T-cell recognition of ovarian cancer. Surgery. 1993;114: 227–34.
30. Peoples GE, Goedegebuure PS, Andrews JV, Schoof DD, Eberlein TJ. HLA-A2 presents shared tumor-associated antigens derived from endogenous proteins in ovarian cancer. J Immunol 1993; 151:5481–91.
31. Castellarin M, Milne K, Zeng T, Tse K, Mayo M, Zhao Y, et al. Clonal evolution of high-grade serous ovarian carcinoma from primary to recurrent disease. J Pathol 2013;229:515–24.
32. Dudley ME, Wunderlich JR, Shelton TE, Even J, Rosenberg SA. Generation of tumor-infiltrating lymphocyte cultures for use in adoptive transfer therapy for melanoma patients. J Immunother 2003;26: 332–42.
33. Warren RL, Choe G, Freeman DJ, Castellarin M, Munro S, Moore R, et al. Derivation of HLA types from shotgun sequence datasets. Genome medicine 2012;4:95.
34. Hoof I, Peters B, Sidney J, Pedersen LE, Sette A, Lund O, et al. NetMHCpan, a method for MHC class I binding prediction beyond humans. Immunogenetics. 2009;61:1–13.
35. Milne K, Barnes RO, Girardin A, Mawer MA, Nesslinger NJ, Ng A, et al. Tumor-infiltrating T cells correlate with NY-ESO-1-specific autoantibodies in ovarian cancer. PLoS ONE 2008;3:e3409.
36. Moodie Z, Price L, Gouttefangeas C, Mander A, Janetzki S, Lower M, et al. Response definition criteria for ELISPOT assays revisited. Cancer Immunol, Immunother 2010;59:1489–501.
37. Bashashati A, Ha G, Tone A, Ding J, Prentice LM, Roth A, et al. Distinct evolutionary trajectories of primary high-grade serous ovarian cancers revealed through spatial mutational profiling. J Pathol 2013;231: 21–34.
38. Cooke SL, Ng CK, Melnyk N, Garcia MJ, Hardcastle T, Temple J, et al. Genomic analysis of genetic heterogeneity and evolution in high-grade serous ovarian carcinoma. Oncogene 2010;29:4905–13.
39. Kiecker F, Streitz M, Ay B, Cherepnev G, Volk HD, Volkmer-Engert R, et al. Analysis of antigen-specific T-cell responses with synthetic peptides—what kind of peptide for which purpose? Hum Immunol 2004;65:523–36.
40. Janetzki S, Panageas KS, Ben-Porat L, Boyer J, Britten CM, Clay TM, et al. Results and harmonization guidelines from two large-scale international Elispot proficiency panels conducted by the Cancer Vaccine Consortium (CVC/SVI). Cancer Immunol Immunother 2008; 57:303–15.
41. Finn OJ. Immuno-oncology: understanding the function and dysfunction of the immune system in cancer. Ann Oncol. 2012;23:viii6-9.
42. Buhrman JD, Slansky JE. Improving T cell responses to modified peptides in tumor vaccines. Immunol Res 2013;55:34–47.
43. Mrass P, Weninger W. Immune cell migration as a means to control immune privilege: lessons from the CNS and tumors. Immunol Rev 2006;213:195–212.
44. Heemskerk B, Kvistborg P, Schumacher TN. The cancer antigenome. Embo J 2013;32:194–203.
45. Motz GT, Coukos G. Deciphering and reversing tumor immune suppression. Immunity 2013;39:61–73.
46. Kandalaft LE, Motz GT, Duraiswamy J, Coukos G. Tumor immune surveillance and ovarian cancer: lessons on immune mediated tumor rejection or tolerance. Cancer Metastasis Rev 2011;30:141–51.
47. Cui TX, Kryczek I, Zhao L, Zhao E, Kuick R, Roh MH, et al. Myeloid-derived suppressor cells enhance stemness of cancer cells by inducing microRNA101 and suppressing the corepressor CtBP2. Immunity 2013;39:611–21.
48. Yi JS, Cox MA, Zajac AJ. T-cell exhaustion: characteristics, causes and conversion. Immunology 2010;129:474–81.
49. Castle JC, Kreiter S, Diekmann J, Lower M, van de Roemer N, de Graaf J, et al. Exploiting the mutanome for tumor vaccination. Cancer Res. 2012;72:1081–91.

CD25 identifies a subset of CD4+FoxP3-TIL that are exhausted yet prognostically favorable in human ovarian cancer

Ronald J. deLeeuw[1,2], David R. Kroeger[1], Sara E. Kost[1,2], Pheh-Ping Chang[1], John R. Webb[1,2], Brad H. Nelson[1,2,3]

[1] Deeley Research Centre, BC Cancer Agency, Victoria BC Canada

[2] Department of Biochemistry and Microbiology, University of Victoria, Victoria BC Canada

[3] Department of Medical Genetics, University of British Columbia, Vancouver BC Canada

Running title: CD25 identifies a prognostically favorable CD4+ TIL subset

Keywords: CD25, CD4, FoxP3, ovarian cancer, tumor-infiltrating lymphocytes, prognosis, multi-color immunohistochemistry

ABSTRACT

CD25, the alpha subunit of the interleukin-2 (IL-2) receptor, is a canonical marker of regulatory T cells (Tregs) and hence has been implicated in immune suppression in cancer. However, CD25 is also required for optimal expansion and activity of effector T cells in peripheral tissues. Thus, we hypothesized that CD25, in addition to demarcating Tregs, might identify effector T cells in cancer. To investigate this, we used multi-parameter flow cytometry and immunohistochemistry to analyze tumor-infiltrating lymphocytes (TIL) in primary high-grade serous carcinomas (HGSC), the most common and fatal subtype of ovarian cancer. CD25 was expressed primarily by CD4+ TIL, with negligible expression by CD8+ TIL. In addition to conventional CD25+FoxP3+ Tregs, we identified a subset of CD25+FoxP3- T cells that comprised up to 13% of CD4+ TIL. In tumors with CD8+ TIL, CD25+FoxP3- T cells showed a strong positive association with patient survival (HR 0.56, P=0.02), which exceeded the negative effect of Tregs (HR 1.55, P=0.09). Amongst CD4+ TIL subsets, CD25+FoxP3- cells expressed the highest levels of PD-1. Moreover, they failed to produce common T helper cytokines (IFN-γ, TNF-α, IL-2, IL-4, IL-10 or IL-17A) after *in vitro* stimulation, suggesting they were functionally exhausted. In contrast, the more abundant CD25-FoxP3- subset of CD4+ TIL expressed low levels of PD-1 and produced T helper 1 cytokines, yet conferred no prognostic benefit. Thus, CD25 identifies a subset of CD4+FoxP3- TIL that, despite being exhausted at diagnosis, have a strong, positive association with patient survival and warrant consideration as effector T cells for immunotherapy.

INTRODUCTION

Studies over the past decade have highlighted the strong influence of the immune system on the survival of cancer patients. In particular, CD8+ tumor-infiltrating lymphocytes (CD8+ TIL) are associated with survival in virtually every human solid cancer studied, including ovarian cancer (1, 2). Importantly, however, CD8+ TIL do not act in isolation but rather through cooperative interactions with other immune cells (3) Thus, to enhance the beneficial effects of TIL, it is imperative to understand how different TIL subsets work together to mediate tumor immunity.

Gooden et al. performed a meta-analysis of 52 studies investigating the prognostic significance of TIL expressing the T cell markers CD3, CD8, CD4 and FoxP3 (4). Intriguingly, CD3+ TIL showed a stronger prognostic effect than CD8+ TIL (pooled hazard ratios of 0.58 and 0.71, respectively), suggesting that other CD3+ TIL, in particular CD4+ T cells, might contribute to favorable prognosis. The prognostic influence of CD4+ TIL has been difficult to assess directly as they include both effector and regulatory subsets (5). Furthermore, CD4 is also expressed by macrophages in humans, thus complicating histopathological scoring (6). Owing to this complexity, CD4 as a standalone marker has shown no association with patient survival in ovarian cancer (7, 8).

CD4+ TIL have been divided into several distinct functional subsets based on cytokine secretion patterns and phenotypic markers (5). For example, IFN-γ-producing CD4+ TIL (Th1 cells) have been identified in ovarian cancer (9), and Th1-like gene expression signatures have been reported as favorable in many cancers (1). More

recently, IL-17-producing CD4+ T cells (Th17 cells) have been identified in several cancers (1). The prognostic effect of Th17 cells appears to depend on tumor site, ranging from unfavorable in colorectal cancer (10) to favorable in ovarian and gastric cancer (11, 12). CD4+ TIL with a regulatory phenotype (Tregs) are also prevalent in human cancer. Tregs are commonly defined by co-expression of the Interleukin-2 Receptor (IL-2R) alpha subunit (CD25) and the transcription factor FoxP3. These cells can inhibit tumor immunity by a variety of mechanisms, including the production of immunosuppressive cytokines, depletion of extracellular ATP, and inhibitory cell contacts (13). Accordingly, Tregs have been associated with poor prognosis in ovarian cancer (8, 14-16) and many other cancer types (1, 17). Thus, CD4+ TIL represent complex mixtures of T cell subsets with both positive and negative influences on tumor immunity.

Although IL-2 can serve as a growth factor for virtually all T cell subsets, Tregs exhibit the most obvious IL-2 dependency *in vivo*. This was revealed most strikingly when IL-2- and IL-2R-deficient mice were first generated. Rather than being immune compromised as many had expected, these animals develop a lethal, systemic autoimmune syndrome that is attributable to the loss of Tregs (18). Thus, CD25 serves not only as a marker of Tregs, but also as a component of an essential developmental and homeostatic signaling pathway for these cells (18). Several strategies have been developed to deplete Tregs in cancer patients by targeting the IL-2 pathway. For example, IL-2 conjugated to diptheria toxin has been used to deplete Tregs *in vivo* (19, 20). Tregs can also be depleted with antibodies to CD25 (21). Although these agents have been shown to reduce the number of circulating Tregs in cancer patients, and improve responses to tumor-specific vaccines, this has generally not resulted in major anti-tumor

effects. Indeed, in the settings of transplantation and autoimmunity, these agents have proven efficacious at inhibiting T cell responses rather than reversing immune suppression (22).

Consistent with this, closer examination of IL-2- or CD25-deficient mice has revealed an important role for IL-2 in the expansion of effector T cells in non-lymphoid tissues such as gut and lung epithelium (23, 24). Moreover, we found in a mouse model of advanced ovarian cancer that IL-2 signaling, though dispensable for the initial expansion of CD8+ T cells, was essential for CD8+ T-cell responses in the tumor environment (25). Indeed, systemic IL-2 infusion can have potent anti-tumor effects as a monotherapy and in the setting of adoptive immunotherapy (26). In ovarian cancer, intraperitoneal IL-2 administration yielded a 25% objective response rate in early phase clinical trials (27, 28). Thus, the physiological role of IL-2 is highly context dependent, and a better understanding of its role in the tumor microenvironment is needed if we are to rationally manipulate this signaling axis.

Toward this end, we evaluated the phenotype and prognostic significance of CD25+ TIL subsets in high-grade serous carcinoma (HGSC), the most common and lethal form of ovarian cancer. In accord with prior reports (8, 14-16), CD4+CD25+FoxP3+ Tregs were a prominent component of CD4+ TIL in many patients, and their presence trended toward decreased patient survival. Unexpectedly, we also identified a CD4+CD25+FoxP3- TIL subset that had a highly exhausted phenotype yet was strongly associated with patient survival. Our results reveal a potentially beneficial role for CD4+CD25+FoxP3- T cells in tumor immunity and provide new insights into immune modulatory strategies for HGSC and related malignancies.

MATERIALS AND METHODS

Patient characteristics and biospecimens

All specimens and clinical data were obtained with either informed written consent or a formal waiver of consent under protocols approved by the Research Ethics Board of the BC Cancer Agency (BCCA) and the University of British Columbia (Vancouver, British Columbia, Canada). All patients in this study were diagnosed with advanced stage, high-grade serous carcinoma (HGSC). Survival analyses were performed with a previously described retrospective cohort comprised of 187 HGSC cases (Table 1) (7, 29). Briefly, a tissue microarray (TMA) with 0.6 mm cores was constructed from formalin-fixed paraffin-embedded tumor samples obtained at the time of primary surgery from patients seen at the BC Cancer Agency from 1984 to 2000 (OvCaRe Ovarian Tumour Bank). Patients in this cohort were deemed optimally de-bulked, meaning they had no macroscopic residual disease.

Flow cytometry studies were performed with viable tumor and blood specimens collected at the time of primary surgery from previously untreated HGSC patients admitted to BCCA from 2007-2010. Tumor tissue samples were mechanically disaggregated in RPMI media containing 0.5 μg/mL collagenase Type I (Sigma-Aldrich, St. Louis, MO), 0.5 μg/mL collagenase Type IV (Sigma-Aldrich, St. Louis, MO), 0.25 μg/mL hyaluronidase (Sigma-Aldrich, St. Louis, MO) and 0.1 μg/mL DNAse I (Sigma-Aldrich, St. Louis, MO) and incubated for 12h at 4^{o} C. Single cell suspensions were prepared by passing digested tissue through a 100 μm filter. Cellular yield and viability

were determined by flow cytometry, and aliquots of 1 x 10^7 cells were frozen in RPMI media containing 50% FBS (Fisher Scientific, Toronto, ON, Canada), and 10% DMSO (Sigma-Aldrich, St. Louis, MO).

Flow cytometry

Tumor cell suspensions were thawed at 37°C followed by washing and a 2 h rest at 37°C in RPMI media (Life Technologies, Burlington, ON, Canada) containing 10% FBS (Fisher Scientific, Toronto, ON, Canada), L-glutamine (Life Technologies, Burlington, ON, Canada), sodium pyruvate (Life Technologies, Burlington, ON, Canada), β-mercaptoethanol (Sigma-Aldrich, St. Louis, MO) and HEPES (Life Technologies, Burlington, ON, Canada). Cells were stained with fluorochrome-conjugated monoclonal antibodies to the following cell surface markers: CD3, CD4, CD8, CD25, CD127, CD357 (GITR), CTLA-4, OX40, LAG-3, PD-1 and TIM-3 (Table S1). To analyze cytokine production and transcription factor expression, bulk tumor preparations were stimulated with phorbol myristate acetate (PMA) (50ng/mL; Sigma-Aldrich, St. Louis, MO) and ionomycin (1μM; Sigma-Aldrich, St. Louis, MO) in the presence of GolgiStop (BD Biosciences, Mississauga, ON, Canada) for 3 h at 37°C. Cells were then fixed and permeabilized with Perm/Fix solution (eBiosciences, San Diego, CA) and stained with fluorochrome-conjugated monoclonal antibodies to IFN-γ, TNF-α, IL-2, IL-4, IL-17, FoxP3 and Helios (Table S1). Flow cytometry was performed using eight-channel Influx or FACSCalibur instruments (BD Biosciences, Mississauga, ON, Canada), and data were analyzed with FlowJo software v10.0.7 (TreeStar Inc., Ashland, OR).

138

139 ***Immunohistochemistry***

140 Multi-color immunohistochemistry (IHC) was performed as previously described
141 (30). Briefly, tumor tissue micro-arrays (TMAs) were stained with pan-cytokeratin alone
142 or the following antibody combinations: (a) CD25, CD8, and FoxP3, and (b) CD3, CD8,
143 and FoxP3 (Table S1). All slides were deparaffinized, treated with Diva Decloaker in a
144 decloaking chamber for antigen-retrieval, and then blocked with Peroxidased-1 and
145 Background Sniper. All staining was performed at room temperature for one hour for the
146 primary antibodies and 30 minutes for secondary amplification. For the pan-cytokeratin
147 stain, the primary signal was amplified using the MACH-2 Mouse-AP polymer kit and
148 visualized with Warp Red (10 minutes). The first antibody combination utilized anti-
149 CD25 (clone 4C9) and anti-CD8a (clone SP16) antibodies, the MACH-2 polymer kit
150 Double Stain 1, and the chromogens Warp Red and Betazoid DAB, respectively. Slides
151 were denaturated at 50°C for 45 minutes to remove the primary and secondary antibodies
152 (31). The anti-CD25 antibody (clone 4C9) was reapplied (to boost the signal) together
153 with the anti-FoxP3 antibody (clone SP97), followed by the secondary polymer kit
154 MACH-2 Double Stain 1 and development with Warp Red and Vina Green, respectively.
155 For the second antibody combination, we used the primary antibodies anti-CD3 (clone
156 SP7) and anti-CD8a (clone C8/144B), the secondary polymer kit MACH-2 Double stain
157 2, and Warp Red and Betazoid DAB, respectively. After denaturation, the second round
158 of staining used anti-FoxP3 antibody (clone SP97), the secondary polymer MACH-2
159 Double Stain 2, and Vina Green. Where indicated, slides were counterstained with

hematoxylin. Other than antibodies (Table S1), all IHC reagents and equipment were obtained from Biocare Medical (Concord, CA).

Image analysis and scoring

Images were captured using an Olympus BX53 microscope equipped with a motorized stage (Quorum technologies Inc, Guelph, ON) and the Nuance™ multispectral imaging system (CRI, Hopkinton, MA). Pan-cytokeratin-stained TMA cores were captured as a single image at 200X magnification. For cores stained with the CD8/CD25/FoxP3 and CD3/CD8/FoxP3 combinations, each chromogen was scanned at its optimal wavelength and 400X magnification. Images were then combined electronically using MetaMorph™ software (Quorum technologies Inc, Guelph, ON). To aid the identification of intraepithelial TIL (as opposed to stromal lymphocytes), cytokeratin-positive tumor regions were overlaid on serial sections stained for TIL markers (Figure S1). To enumerate TIL, multi-spectral images were deconvoluted into individual components using Nuance™ software. Using Metamorph™ software (Quorum technologies Inc, Guelph, ON) images containing three chromogens were re-created and used to visually count cells with the indicated phenotypes.

Cases were considered positive for a given TIL subset if at least one cell was present per 0.6 mm core. The density of each intraepithelial TIL subset was calculated by normalizing cell counts by epithelial area as defined by positive cytokeratin staining on a neighboring tissue section. The mean number of CD25-FoxP3- TIL was inferred for the cohort by subtracting the mean number of CD8-CD25+FoxP3- T cells seen with the

CD25/CD8/FoxP3 IHC combination from the mean number of CD3+CD8-FoxP3- T cells seen with CD3/CD8/FoxP3 combination.

Statistical analysis

All statistical analyses were performed using GraphPad Prism 6.0. Survival analysis was performed using Kaplan-Meier plots and log-rank tests. Pearson correlations were used to assess associations between TIL subsets. Chi-squared analysis was used to assess the association of TIL subsets with MHC class II. P values of less than 0.05 were considered significant.

RESULTS

CD25 and FoxP3 define four subsets of CD4+ TIL

To assess which populations of TIL express CD25, we performed multi-parameter flow cytometry on disaggregated tumor samples from 12 HGSC patients. CD25 was expressed by a small but significant proportion of CD3+ TIL (mean 12%, range 3-20%) and was not found on any non-T (CD3-) cells. The majority of CD25+ T cells were CD4+CD8- (mean 84%, range 78-91%), and a small proportion were CD4-CD8+ (mean 3%, range 1-7%) (Figure 1A, D). The remaining CD25+ cells were CD4-CD8- or CD4+CD8+. Amongst CD4+ TIL, CD25 was expressed by an average of 20% of cells (range 4-28%) (Figure 1B, D). To investigate whether these were Tregs, we stained for the transcription factor FoxP3. Consistent with prior reports (8, 14-16), cells with a canonical Treg phenotype (CD25+FoxP3+) constituted a significant fraction of CD4+ TIL (mean 13%, range 3-25%) and are hereafter referred to as Tregs. Notably, a substantial fraction of CD25+ TIL did not express FoxP3 (mean 7%, range 2-13%) (Figure 1C, D). The remaining CD4+ TIL were CD25-FoxP3+ (mean 7%) or CD25-FoxP3- (mean 74%) (Figure 1C, D). Amongst CD8+ TIL, only a small percentage expressed CD25 (mean <1%), FoxP3 (mean 2%) or both (mean <1%) (data not shown). Similar T cell subsets were found in peripheral blood samples from healthy donors except that CD4+CD25+FoxP3- T cells were rare and CD4+CD25-FoxP3+ T cells were notably absent (data not shown).

Prognostic significance of TIL subsets

To investigate the prognostic significance of TIL subsets, a 187-case HGSC TMA was stained with antibodies to CD8, CD25 and FoxP3 (Figure 2A). Because CD4 is also expressed by macrophages (6), it is difficult to score CD4+ TIL directly. Instead, we assumed that any CD25+ and/or FoxP3+ cell that did not express CD8 was a CD4+ T cell, an assumption that was justified by the above flow cytometry results (Figure 1). With this staining combination, we could directly visualize all CD8+ TIL subsets, as well as the CD25+FoxP3-, CD25+FoxP3+ and CD25-FoxP3+ subsets of CD4+ TIL. To infer the number of CD4+CD25-FoxP3- TIL, we employed a second IHC combination involving antibodies to CD3, CD8 and FoxP3. We determined the number of CD4+FoxP3- cells, which appeared as CD3+CD8-FoxP3- cells. From this, we subtracted the number of CD25+FoxP3- cells determined from the first staining combination. This yielded an estimate of the number of CD4+CD25-FoxP3- cells. Our detection and scoring approach proved valid, as the results obtained by multi-color IHC and flow cytometry were concordant (Fig. 1D, E). We stained an adjacent section of the TMA for cytokeratin to unequivocally identify tumor epithelium versus stroma; for all subsequent analyses we focused on intraepithelial TIL, as these have the greatest prognostic significance (2).

A large proportion of cases (74%) scored positive for CD8+ TIL (Figure 2B), and consistent with the flow cytometry data, only a small number of CD8+ TIL expressed CD25 and/or FoxP3 (data not shown). With few exceptions, cases with CD8+ TIL also had CD4+ TIL (defined as CD3+CD8- cells), and conversely, almost all cases with CD4+ TIL also had CD8+ TIL (Figure 2B). Thus, CD8+ and CD4+ TIL were strongly associated with one another. Tregs (defined as CD8-CD25+FoxP3+ cells) were the most

prevalent subset of CD4+ TIL, being present in 67% of cases (Figure 2B). The CD25+FoxP3- and CD25-FoxP3+ subsets were present in 55% and 43% of cases, respectively (Figure 2B). Thus, the different subsets of CD4+ TIL were usually found together, although there were exceptions. All subsets of CD4+ TIL showed a strong association with MHC class II expression by tumor cells (determined in a previous study of this cohort (7)) ($P<0.01$ for all subsets).

As expected, CD8+ TIL were strongly associated with disease-specific survival (HR = 0.33, P-value<0.0001; not shown) and progression free survival (HR = 0.38, P-value<0.0001) (Figure 3A). The strong prognostic effect of CD8+ TIL can confound the analysis of closely associated TIL subsets, such as Tregs (30). Therefore, to determine the prognostic significance of CD4+ TIL subsets, we restricted our analysis to cases that were positive for CD8+ TIL. As expected, cases with a higher than median ratio of Tregs to CD8+ TIL trended toward decreased survival (HR = 1.55, P-value=0.09) (Figure 3B). In contrast, a higher than median ratio of CD25+FoxP3- TIL to CD8+ TIL was strongly associated with survival (HR = 0.56, P-value=0.02) (Fig. 3C). The prognostic effect of CD25+FoxP3- TIL was even more pronounced in cases with lower levels of Tregs (HR = 0.29, P-value=0.003) (Figure 3D). No other CD4+ TIL subsets showed an association with survival (Figure 3E, F). Thus, the CD25+FoxP3- subset was unique among CD4+ TIL in showing a positive association with patient survival.

CD25+Foxp3- T cells are phenotypically distinct from other TIL subsets

To better understand the prognostic effect of CD25+FoxP3- TIL, we used multi-color flow cytometry to assess their activation status and cytokine production profile in

comparison to other CD4+ TIL subsets (n = 6 cases; Figure 4A). CD25+FoxP3- TIL had an activated phenotype as evidenced by high CD69 and low CCR7 expression (Figure S2B). In comparison to Tregs, CD25+FoxP3- TIL expressed similar levels of GITR; however, they expressed lower levels of CTLA-4 and OX40 and were negative for Helios (Figure 4B). These data suggested that CD25+FoxP3- cells might be Th1 cells, which are widely reported among TIL (1). Unexpectedly, however, CD25-+FoxP3- T cells failed to produce any of the hallmark Th1 cytokines IFN-γ, TNF-α or IL-2 after *in vitro* stimulation with PMA and ionomycin (Figure 4C). Indeed, Th1 cytokines were only produced by the CD25-FoxP3- subset (Figure 4C). None of the CD4+ TIL subsets produced IL-4 or IL-17A (Figure S2D).

Given that CD25+FoxP3- T cells did not express canonical Th cytokines, we investigated the possibility that they might represent other less common CD4+ T cell phenotypes. CD4+ cytolytic T cells have been described in cancer (32); however, similar to other non-Treg cells, very few CD25+FoxP3- T cells expressed the cytolytic markers TIA-1, granzyme B or perforin (Figure S2E). Furthermore, CD25+FoxP3- TIL did not express CXCR5, a marker of T follicular helper cells (Figure S2F).

Based on their lack of discernible functional attributes, we hypothesized that CD25+FoxP3-TIL might be in a suppressed or exhausted state. In accord with this, we found that CD25+FoxP3- T cells expressed very high levels of the exhaustion marker PD-1 (Figure 4D). Indeed, the level of PD-1 expressed by CD25+FoxP3- TIL was on average 3.1-fold higher than Tregs, and 6.6-fold higher than CD25-FoxP3- cells. In addition, CD25+FoxP3- TIL expressed the exhaustion markers LAG-3 (Figure S2G) and TIM-3, the latter being found on cells with the highest PD-1 levels (Figure 4D). Thus,

despite being prognostically favorable, CD25+FoxP3- TIL exhibited an exhausted phenotype based on the expression of these markers and deficient cytokine production.

DISCUSSION

Using multi-parameter flow cytometry and immunohistochemistry, we have shown that CD25 and FoxP3 delineate four subsets of CD4+ TIL with distinct functional and prognostic attributes. Consistent with prior reports (8, 14-16), CD25+FoxP3+ Tregs constituted a substantial proportion of CD4+ TIL, expressed canonical Treg markers (Helios, CTLA-4 and OX40), and showed a trend toward decreased patient survival. CD25-FoxP3- T cells constituted the largest subset of CD4+ TIL and were the sole source of Th1 cytokines; however, despite their abundance and functional competence, these cells conferred no apparent prognostic benefit. Instead, the CD25+FoxP3- subset showed a strong association with patient survival, despite expressing very high levels of PD-1 and failing to produce cytokines. This paradoxical relationship between functional status and prognosis might be explained by the fact that PD-1 is a marker of tumor-reactive TIL (33, 34). Thus, the exhausted state of CD25+FoxP3- TIL observed here might reflect ongoing recognition of tumor antigens. Although speculative, this state of exhaustion might subsequently be relieved by the cytoreductive and immune stimulatory effects of surgery and chemotherapy (35), ultimately leading to increased patient survival. Thus, CD25+FoxP3- TIL warrant further investigation for their contribution to spontaneous tumor immunity as well as their potential to serve as effector cells for immunotherapy.

CD25+FoxP3- T cells have been largely overlooked in prior studies of CD4+ TIL, likely because of their low abundance and failure to make cytokines typical of Th1, Th2, Th17, or Tregs. Adding to their inconspicuous nature, these cells are very rare in PBMC and hence would not be obvious in blood-based immune analyses. Nonetheless, cells with this phenotype are evident in published data of CD4+ TIL in ovarian (14, 36, 37), and other tumors (38). Moreover, their prognostic significance has been directly assessed in one prior study of HGSC. Preston et al. used multi-color IHC to enumerate CD4+CD25+FoxP3- TIL in HGSC patients who had demonstrated long (>18 months) versus short survival (8). Although these cells were equally abundant in the two groups, the ratio of CD8+ to CD4+CD25+FoxP3- TIL was modestly higher in the long survival group (0.65 versus 0.46), leading the authors to propose that CD25+FoxP3- TIL play an inhibitory role in tumor immunity. However, this interpretation could potentially reflect a confounding effect of CD8+ TIL. Specifically, cases exhibiting a low ratio of CD8+ to CD25+FoxP3- TIL were undoubtedly enriched for tumors with few or no CD8+ TIL, which itself is a poor prognostic factor (2). We attempted to correct for this effect by restricting our survival analysis to cases that were positive for CD8+ TIL, thereby allowing us to assess any additional prognostic effects contributed by the different CD4+ TIL subsets. The validity of this approach was supported by our finding that, with few exceptions, CD25+FoxP3- TIL were found only in cases with CD8+ TIL (Figure 2B). With this correction, a strong positive prognostic effect of CD25+FoxP3+ TIL was revealed.

To explain this positive effect, we propose that CD25+FoxP3- TIL might be tumor-reactive T helper cells that have become functionally impaired or exhausted due to

chronic antigen exposure. Indeed, their appearance on flow cytometric plots initially suggested to us that they might represent a $CD25^{hi}$ "shoulder" of the Th1-like CD25-FoxP3- subset. To address this, we assessed the prognostic significance of CD3+CD8-FoxP3- TIL, a grouping that included both the CD25-FoxP3- and CD25+FoxP3- subsets. CD3+CD8-FoxP3- TIL showed no prognostic significance, indicating that the positive effect of CD25+FoxP3- TIL was lost when combined with CD25-FoxP3- TIL (Figure 3F). Although an indirect assessment, this indicates that CD25-FoxP3- TIL have negligible (or possibly even negative) prognostic significance and that CD25+FoxP3- TIL make a unique positive contribution to tumor immunity.

At first glance, the above findings may appear inconsistent with prior studies reporting that TIL with Th1, Th17 or other cytokine patterns are prognostically favorable in ovarian (39, 40) and other cancers (1). However, many of these prior studies were based on the analysis of bulk tumor samples for expression of Th1-associated genes such as IFN-γ, TNF-α, T-bet, IRF-1 and STAT4 (10, 39, 40). Notably, these genes are also expressed by CD8+ T cells and NK cells; therefore, gene expression analysis of bulk tumor tissue does not reveal the prognostic influence of CD4+ Th1 cells *per se*. Using a flow cytometric approach, Kryczek et al. showed that production of IFN-γ, IL-2, TNF-α and IL-17 by CD4+ TIL was restricted to CD25-, FoxP3-, and $PD\text{-}1^{lo}$ cells and that IL-17 levels in ascites fluid were associated with survival . In accord with their results, we found that cytokine production was restricted to the CD25-/FoxP3-/$PD\text{-}1^{lo}$ subset; however, we failed to detect IL-17 production by any CD4+ TIL subset. This might reflect a low abundance of Th17 cells in ovarian cancer (as others have also reported (37, 41), or inadequate sensitivity of our flow cytometric assay for IL-17 production. Finally,

two studies have used MHC class II tetramers specific for the tumor antigen NY-ESO-1 to isolate CD4+ T cells from peripheral blood (42) or tumors (9) of ovarian cancer patients. NY-ESO-1-specific T cells were found to produce Th1-associated cytokines after *in vitro* stimulation. However, the Th1 competence of these T cells may reflect the fact that they were derived from peripheral blood, which has negligible CD25+FoxP3- T cells, or expanded *in vitro* by PHA stimulation, which can reverse T cell exhaustion. From a broader perspective, our data does not contradict the notion that a Th1-like tumor environment is favorable for patient prognosis. Indeed, it is conceivable that CD25+FoxP3- TIL have an intrinsic Th1 phenotype that is obscured by PD-1-mediated exhaustion.

Although CD25 is a well-established marker of Tregs, to our knowledge this is the first report of CD25 expression by T cells with an exhausted phenotype. This observation may lead to further insights into the signaling state of CD25+FoxP3- TIL, as the mechanisms of transcriptional regulation of the CD25 gene are relatively well characterized. The CD25 promoter has both positive and negative regulatory elements, which bind multiple factors including NFAT, NF-κB, STAT5 and SMAD3/4 (43). Transient CD25 expression is induced on virtually all T cells by activation of the TCR and the downstream NFAT and NF-κB pathways (43). CD25 can also be induced by a variety of cytokines, including IL-1, IL-2, IL-7, IL-12, IL-15, TNF-α and TGF-β (43). In particular, IL-2 induces CD25 expression via STAT5 (43) and in combination with extensive antigen stimulation induces expression of Blimp-1, which also upregulates CD25 expression (18), Finally, CD25 is expressed at high, constitutive levels by Tregs through a combination of TCR signaling, IL-2-induced STAT5 activation, and

constitutive expression of FoxP3 (18). In the case of CD25+FoxP3- TIL, this FoxP3-dependent mechanism would not apply. Rather, CD25 might be induced by antigen stimulation in combination with IL-2, a cytokine for which they would be competitive consumers based on their $CD25^{hi}$ phenotype. Another candidate is TGF-β, which can induce CD25 (44) and is present in most epithelial tumors. In this regard, it is noteworthy that CD25+FoxP3- cells expressed high levels of PD-1, which is also induced by TCR stimulation in combination with TGF-β (45). One paradoxical aspect of the phenotype of CD25+FoxP3- cells is that they somehow maintain CD25 expression despite high levels of PD-1, which normally blunts TCR signaling through SHP-2-mediated dephosphorylation of ZAP70 (46). This suggests that CD25 might be relatively insensitive to PD-1-mediated inhibition, as described for other gene products (47).

The findings reported here have implications for the development of effective immunotherapies for HGSC and related cancers. First, our data indicates that strategies to deplete Tregs by targeting CD25 might have the detrimental effect of also eliminating CD25+FoxP3- T cells. Indeed, in renal transplantation and autoimmunity, the net effect of anti-CD25 antibody therapy is immune suppression not activation (22). Second, our findings might help to explain the positive clinical effects of IL-2 in ovarian cancer, where a 25% response rate was achieved with intraperitoneal administration of IL-2 as a monotherapy (26). Third, our data has implications for checkpoint blockade strategies. As many CD25+FoxP3- TIL express high levels of CTLA-4 (Figure 4B), antibodies to CTLA-4 might inadvertently deplete this subset (48). On the other hand, our data supports further investigation of PD-1 blockade in HGSC, given that CD25+FoxP3- TIL expressed the highest levels of PD-1 compared to all other CD4+ TIL subsets (Figure

398 4D). Finally, our data reveals OX40 as a promising target for immune modulation, since
399 this molecule was highly expressed by Tregs but not the other three CD4+ TIL subsets
400 (Figure 4B). While antibodies to OX40 can directly stimulate effector T cells (38, 49),
401 they can also enhance antitumor immunity by depleting OX40+ Tregs (50). In summary,
402 our study highlights the IL-2, PD-1 and OX40 pathways as potential immunotherapeutic
403 targets to differentially enhance the positive effects of CD25+FoxP3- TIL over the
404 inhibitory effects of Tregs.
405

406 **ACKNOWLEDGEMENTS**

407 We thank the donors and clinicians who provided specimens for our research, and
408 Peter Watson and Katy Milne for technical advice.
409

410 **GRANT SUPPORT**

411 This study was supported by the Canadian Institutes of Health Research
412 (MOP97897 and a fellowship to RJD), U.S. Department of Defense (OC110435), BC
413 Cancer Foundation, and the BC Cancer Agency Tumour Tissue Repository, a member of
414 the Canadian Tumour Repository Network.

REFERENCES

1. Fridman WH, Pages F, Sautes-Fridman C, Galon J. The immune contexture in human tumours: impact on clinical outcome. Nat Rev Cancer 2012; 12: 298-306.
2. Hwang WT, Adams SF, Tahirovic E, Hagemann IS, Coukos G. Prognostic significance of tumor-infiltrating T cells in ovarian cancer: a meta-analysis. Gynecol Oncol 2012; 124: 192-8.
3. Bindea G, Mlecnik B, Tosolini M, et al. Spatiotemporal dynamics of intratumoral immune cells reveal the immune landscape in human cancer. Immunity 2013; 39: 782-95.
4. Gooden MJ, de Bock GH, Leffers N, Daemen T, Nijman HW. The prognostic influence of tumour-infiltrating lymphocytes in cancer: a systematic review with meta-analysis. Br J Cancer 2011; 105: 93-103.
5. Kim HJ, Cantor H. CD4 T-cell subsets and tumor immunity: the helpful and the not-so-helpful. Cancer Immunol Res 2014; 2: 91-8.
6. Crocker PR, Jefferies WA, Clark SJ, Chung LP, Gordon S. Species heterogeneity in macrophage expression of the CD4 antigen. J Exp Med 1987; 166: 613-8.
7. Milne K, Kobel M, Kalloger SE, et al. Systematic analysis of immune infiltrates in high-grade serous ovarian cancer reveals CD20, FoxP3 and TIA-1 as positive prognostic factors. PLoS One 2009; 4: e6412.
8. Preston CC, Maurer MJ, Oberg AL, et al. The ratios of CD8+ T cells to CD4+CD25+ FOXP3+ and FOXP3- T cells correlate with poor clinical outcome in human serous ovarian cancer. PLoS One 2013; 8: e80063.
9. Ayyoub M, Pignon P, Classe JM, Odunsi K, Valmori D. CD4+ T effectors specific for the tumor antigen NY-ESO-1 are highly enriched at ovarian cancer sites and coexist with, but are distinct from, tumor-associated Treg. Cancer Immunol Res 2013; 1: 303-8.
10. Tosolini M, Kirilovsky A, Mlecnik B, et al. Clinical impact of different classes of infiltrating T cytotoxic and helper cells (Th1, th2, treg, th17) in patients with colorectal cancer. Cancer Res 2011; 71: 1263-71.
11. Kryczek I, Banerjee M, Cheng P, et al. Phenotype, distribution, generation, and functional and clinical relevance of Th17 cells in the human tumor environments. Blood 2009; 114: 1141-9.
12. Chen JG, Xia JC, Liang XT, et al. Intratumoral expression of IL-17 and its prognostic role in gastric adenocarcinoma patients. Int J Biol Sci 2011; 7: 53-60.
13. Josefowicz SZ, Lu LF, Rudensky AY. Regulatory T cells: mechanisms of differentiation and function. Annu Rev Immunol 2012; 30: 531-64.
14. Curiel TJ, Coukos G, Zou L, et al. Specific recruitment of regulatory T cells in ovarian carcinoma fosters immune privilege and predicts reduced survival. Nat Med 2004; 10: 942-9.
15. Sato E, Olson SH, Ahn J, et al. Intraepithelial CD8+ tumor-infiltrating lymphocytes and a high CD8+/regulatory T cell ratio are associated with favorable prognosis in ovarian cancer. Proc Natl Acad Sci U S A 2005; 102: 18538-43.
16. Shah CA, Allison KH, Garcia RL, Gray HJ, Goff BA, Swisher EM. Intratumoral T cells, tumor-associated macrophages, and regulatory T cells: association with p53

mutations, circulating tumor DNA and survival in women with ovarian cancer. Gynecol Oncol 2008; 109: 215-9.
17. deLeeuw RJ, Kost SE, Kakal JA, Nelson BH. The prognostic value of FoxP3+ tumor-infiltrating lymphocytes in cancer: a critical review of the literature. Clin Cancer Res 2012; 18: 3022-9.
18. Malek TR, Castro I. Interleukin-2 receptor signaling: at the interface between tolerance and immunity. Immunity 2010; 33: 153-65.
19. Dannull J, Su Z, Rizzieri D, et al. Enhancement of vaccine-mediated antitumor immunity in cancer patients after depletion of regulatory T cells. J Clin Invest 2005; 115: 3623-33.
20. Morse MA, Hobeika AC, Osada T, et al. Depletion of human regulatory T cells specifically enhances antigen-specific immune responses to cancer vaccines. Blood 2008; 112: 610-8.
21. Rech AJ, Vonderheide RH. Clinical use of anti-CD25 antibody daclizumab to enhance immune responses to tumor antigen vaccination by targeting regulatory T cells. Ann N Y Acad Sci 2009; 1174: 99-106.
22. Milo R. The efficacy and safety of daclizumab and its potential role in the treatment of multiple sclerosis. Ther Adv Neurol Disord 2014; 7: 7-21.
23. D'Souza WN, Schluns KS, Masopust D, Lefrancois L. Essential role for IL-2 in the regulation of antiviral extralymphoid CD8 T cell responses. J Immunol 2002; 168: 5566-72.
24. D'Souza WN, Lefrancois L. IL-2 is not required for the initiation of CD8 T cell cycling but sustains expansion. J Immunol 2003; 171: 5727-35.
25. Yang T, Wall EM, Milne K, Theiss P, Watson P, Nelson BH. CD8+ T cells induce complete regression of advanced ovarian cancers by an interleukin (IL)-2/IL-15 dependent mechanism. Clin Cancer Res 2007; 13: 7172-80.
26. Rosenberg SA. IL-2: the first effective immunotherapy for human cancer. J Immunol 2014; 192: 5451-8.
27. Edwards RP, Gooding W, Lembersky BC, et al. Comparison of toxicity and survival following intraperitoneal recombinant interleukin-2 for persistent ovarian cancer after platinum: twenty-four-hour versus 7-day infusion. J Clin Oncol 1997; 15: 3399-407.
28. Vlad AM, Budiu RA, Lenzner DE, et al. A phase II trial of intraperitoneal interleukin-2 in patients with platinum-resistant or platinum-refractory ovarian cancer. Cancer Immunol Immunother 2009; 59: 293-301.
29. Clarke B, Tinker AV, Lee CH, et al. Intraepithelial T cells and prognosis in ovarian carcinoma: novel associations with stage, tumor type, and BRCA1 loss. Mod Pathol 2009; 22: 393-402.
30. West NR, Kost SE, Martin SD, et al. Tumour-infiltrating FOXP3(+) lymphocytes are associated with cytotoxic immune responses and good clinical outcome in oestrogen receptor-negative breast cancer. Br J Cancer 2012; 108: 155-62.
31. Pirici D, Mogoanta L, Kumar-Singh S, et al. Antibody elution method for multiple immunohistochemistry on primary antibodies raised in the same species and of the same subtype. J Histochem Cytochem 2009; 57: 567-75.
32. Tran E, Turcotte S, Gros A, et al. Cancer immunotherapy based on mutation-specific CD4+ T cells in a patient with epithelial cancer. Science 2014; 344: 641-5.

33. Ahmadzadeh M, Johnson LA, Heemskerk B, et al. Tumor antigen-specific CD8 T cells infiltrating the tumor express high levels of PD-1 and are functionally impaired. Blood 2009; 114: 1537-44.
34. Gros A, Robbins PF, Yao X, et al. PD-1 identifies the patient-specific CD8(+) tumor-reactive repertoire infiltrating human tumors. J Clin Invest 2014; 124: 2246-59.
35. Kroemer G, Galluzzi L, Kepp O, Zitvogel L. Immunogenic cell death in cancer therapy. Annu Rev Immunol 2013; 31: 51-72.
36. Kryczek I, Liu R, Wang G, et al. FOXP3 defines regulatory T cells in human tumor and autoimmune disease. Cancer Res 2009; 69: 3995-4000.
37. Leveque L, Deknuydt F, Bioley G, et al. Interleukin 2-mediated conversion of ovarian cancer-associated CD4+ regulatory T cells into proinflammatory interleukin 17-producing helper T cells. J Immunother 2009; 32: 101-8.
38. Curti BD, Kovacsovics-Bankowski M, Morris N, et al. OX40 is a potent immune-stimulating target in late-stage cancer patients. Cancer Res 2013; 73: 7189-98.
39. Kusuda T, Shigemasa K, Arihiro K, Fujii T, Nagai N, Ohama K. Relative expression levels of Th1 and Th2 cytokine mRNA are independent prognostic factors in patients with ovarian cancer. Oncol Rep 2005; 13: 1153-8.
40. Marth C, Fiegl H, Zeimet AG, et al. Interferon-gamma expression is an independent prognostic factor in ovarian cancer. Am J Obstet Gynecol 2004; 191: 1598-605.
41. Fialova A, Partlova S, Sojka L, et al. Dynamics of T-cell infiltration during the course of ovarian cancer: the gradual shift from a Th17 effector cell response to a predominant infiltration by regulatory T-cells. Int J Cancer 2012; 132: 1070-9.
42. Redjimi N, Duperrier-Amouriaux K, Raimbaud I, et al. NY-ESO-1-specific circulating CD4+ T cells in ovarian cancer patients are prevalently T(H)1 type cells undetectable in the CD25+ FOXP3+ Treg compartment. PLoS One 2011; 6: e22845.
43. Liao W, Lin JX, Leonard WJ. Interleukin-2 at the crossroads of effector responses, tolerance, and immunotherapy. Immunity 2013; 38: 13-25.
44. Kim HP, Kim BG, Letterio J, Leonard WJ. Smad-dependent cooperative regulation of interleukin 2 receptor alpha chain gene expression by T cell receptor and transforming growth factor-beta. J Biol Chem 2005; 280: 34042-7.
45. Park B, Chattergoon M, Pan F, Pardoll D, Cox A. TGF-β1 enhances T-cell PD-1 expression through a Smad3-dependant increase in transcription. (IRM4P.499) The Journal of Immunology; 2014. p. 1 Supplement-61.6.
46. Okazaki T, Chikuma S, Iwai Y, Fagarasan S, Honjo T. A rheostat for immune responses: the unique properties of PD-1 and their advantages for clinical application. Nat Immunol 2013; 14: 1212-8.
47. Wei F, Zhong S, Ma Z, et al. Strength of PD-1 signaling differentially affects T-cell effector functions. Proc Natl Acad Sci U S A 2013; 110: E2480-9.
48. Simpson TR, Li F, Montalvo-Ortiz W, et al. Fc-dependent depletion of tumor-infiltrating regulatory T cells co-defines the efficacy of anti-CTLA-4 therapy against melanoma. J Exp Med 2013; 210: 1695-710.
49. Moran AE, Kovacsovics-Bankowski M, Weinberg AD. The TNFRs OX40, 4-1BB, and CD40 as targets for cancer immunotherapy. Curr Opin Immunol 2013; 25: 230-7.

50. Valzasina B, Guiducci C, Dislich H, Killeen N, Weinberg AD, Colombo MP. Triggering of OX40 (CD134) on CD4(+)CD25+ T cells blocks their inhibitory activity: a novel regulatory role for OX40 and its comparison with GITR. Blood 2005; 105: 2845-51.

TABLES

Table 1. *Clinical characteristics of the retrospective HGSC cohort.*

N=187			**Univariate P-value**
Disease Specific Survival (years)	Median	6.6	
Age (years)	median (range)	60.0 (37.6-85.9)	0.16
FIGO Stage	I	47 (25%)	<0.0001
	II	76 (41%)	
	III	64 (34%)	
Grade	G2	52 (28%)	0.55
	G3	135 (72%)	

Table S1. Antibodies used in this study.

Flow-cytometry		
Antigen	**Clone**	**Source**
CD127	eBioRDR5	eBioscience
CD25	M-A251	BD Pharmingen
CD3	UCHT1	BD Horizon
CD3	OKT3	eBioscience
CD4	RPA-T4	BD Horizon
CD4	OKT4	Biolegend
CD45RO	UCHL1	eBioscience
CD69	FN50	eBioscience
CD8a	RPA-T8	BD Horizon
CD8a	RPA-T8	Biolegend
CTLA-4	L3D10	Biolegend
CXCR5	RF8B2	BD Horizon
FoxP3	236A/E7	eBioscience
GITR	eBioAITR	eBioscience
Granzyme B	GB11	BD Horizon
Helios	22F6	Biolegend
IFN-γ	B27	BD Pharmingen
IL-17A	eBio4DEC17	eBioscience
IL-2	MQ1-17H12	BD Pharmingen
IL-4	MP4-25D2	BD Pharmingen
LAG-3	17B4	Enzo
PD-1	EH12.2H7	Biolegend
Perforin	G289-1	BD Pharmingen
TIA-1	IM3293	Beckman Coulter
TIM-3	F38-2E2	eBioscience
TNF-α	MAb11	BD Pharmingen
Immunohistochemistry		
Antigen	**Clone**	**Source**
CD25	4C9	Lab Vision
CD3	SP7	Spring Bioscience
CD8a	C8/144B	Cell Marque
CD8a	SP16	Spring Bioscience
Pan-cytokeratin	OSCAR	Cell Marque
FoxP3	SP79	Spring Bioscience

FIGURE LEGENDS

Figure 1. ***CD25 and FoxP3 define four subsets of CD4+ TIL***. Multi-parameter flow-cytometry was performed on bulk disaggregated tumor samples from 12 HGSC patients, and data is shown for one representative case. **(A)** CD25+ TIL consisted predominantly of CD3+CD4+ T cells. **(B)** Approximately 20% of CD3+CD4+ TIL expressed CD25. **(C)** Within the population of CD3+CD4+ TIL, expression of CD25 and FoxP3 defined four subsets, indicated by the quadrants. **(D)** Average proportions of the four CD4+ TIL subsets (+/- range) for the 12 cases analyzed by flow cytometry. **(E)** Average proportions of the four CD4+ TIL subsets (+/- standard error mean [SEM]) for 181 evaluable cores of the TMA analyzed by multi-color IHC. For the flow cytometry experiments in panels A-D, events were gated on live cells with forward and side scatter characteristics of lymphocytes. The numbers shown indicate the percentage of events falling within an indicated gate.

Figure 2. ***Analysis of TIL subsets by multicolor immunohistochemistry and spectral image analysis***. A 187-case TMA was triple stained with antibodies to CD8, CD25 and FoxP3 and counterstained with hematoxylin. **(A)** Brightfield (upper left panel) and pseudo-colored images from a representative tumor core showing examples of four TIL subsets: (a) CD8-CD25+FoxP3+, (b) CD8+CD25-FoxP3-, (c) CD8-CD25-FoxP3+, and (d) CD8-CD25+FoxP3+. Magnification, 400X. **(B)** Venn diagram showing the distribution of the five indicated TIL subsets, with numbers indicating the percentage of cases scoring positive for each TIL subset.

Figure 3. ***Prognostic significance of TIL subsets***. Kaplan-Meier plots showing the association between TIL subsets and progression free-survival. **(A)** Density of intraepithelial CD8+ TIL. **(B)** Ratio of CD25+FoxP3+ to CD8+ TIL. **(C)** Ratio of CD25-FoxP3+ to CD8+ TIL. **(D)** Ratio of CD25+FoxP3- to CD8+ TIL. **(E)** Ratio of CD4+ (i.e., CD3+CD8-) to CD8+ TIL. **(F)** Cases were stratified into two groups: above median CD25+FoxP3:CD8+ ratio and below median CD25+FoxP3+:CD8+ ratio (n=26) versus below median CD25+FoxP3:CD8+ ratio and above median CD25+FoxP3+:CD8+ ratio (n=26). In each panel, log-rank tests were used to determine P-values, and hazard ratios (HR) are shown for each analysis. For panels B-F, analyses were restricted to cases that were positive for CD8+ TIL.

Figure 4. ***Phenotype and functional characteristics of CD4+ TIL subsets.*** Multi-parameter flow cytometry was used to assess expression of the indicated activation and differentiation markers and cytokines for four CD4+ T cell subsets defined by CD25 and FoxP3 expression. **(A)** Contour plot showing four CD4+ TIL subsets and color scheme used in other panels: CD25+FoxP3- (red), CD25+FoxP3+ (orange), CD25-FoxP3- (blue), CD25-FoxP3+ (green). **(B)** Expression of T cell activation and differentiation markers by the four TIL subsets. **(C)** Cytokine production after 3 hours of stimulation with PMA and ionomycin. **(D)** Expression of exhaustion markers (note that the right panel shows only the CD25+FoxP3- and CD25-FoxP3- subsets). Data is shown for one representative case from a total of six.

Supplementary Figure S1. ***Pan-cytokeratin immunohistochemistry to define regions of tumor epithelium versus stroma.*** TMA sections adjacent to those used for TIL subset analysis were stained with a pan-cytokeratin antibody and counterstained with hematoxylin. **(A)** Epithelial regions as defined by cytokeratin staining are outlined. **(B)** Outlines of epithelial regions were overlaid on multicolor IHC images to facilitate counting of intraepithelial TIL.

Supplementary Figure S2. ***Additional phenotype and functional characteristics of CD4+ TIL subsets.*** This figure shows additional data from the experiment presented in Figure 4. For convenience, it also shows the data from Figure 4. Multi-parameter flow cytometry was used to assess expression of the indicated activation and differentiation markers and cytokines for four CD4+ T cell subsets defined by CD25 and FoxP3 expression. **(A)** Contour plot showing four CD4+ TIL subsets and color scheme used in other panels: CD25+FoxP3- (red), CD25+FoxP3+ (orange), CD25-FoxP3- (blue), CD25-FoxP3+ (green). **(B)** T cell activation markers. **(C)** Treg markers. **(D)** Cytokine production after 3 hours of stimulation with PMA and ionomycin. **(E)** Cytotoxity markers **(F)** CXCR5, a marker of T follicular helper (Tfh) cells. **(G)** Exhaustion markers (note that the right panel shows only the CD25+FoxP3- and CD25-FoxP3- subsets). Dotted lines in panel G represent staining on healthy donor CD3+CD4+ PBMC. Data is shown for one representative case from a total of six.

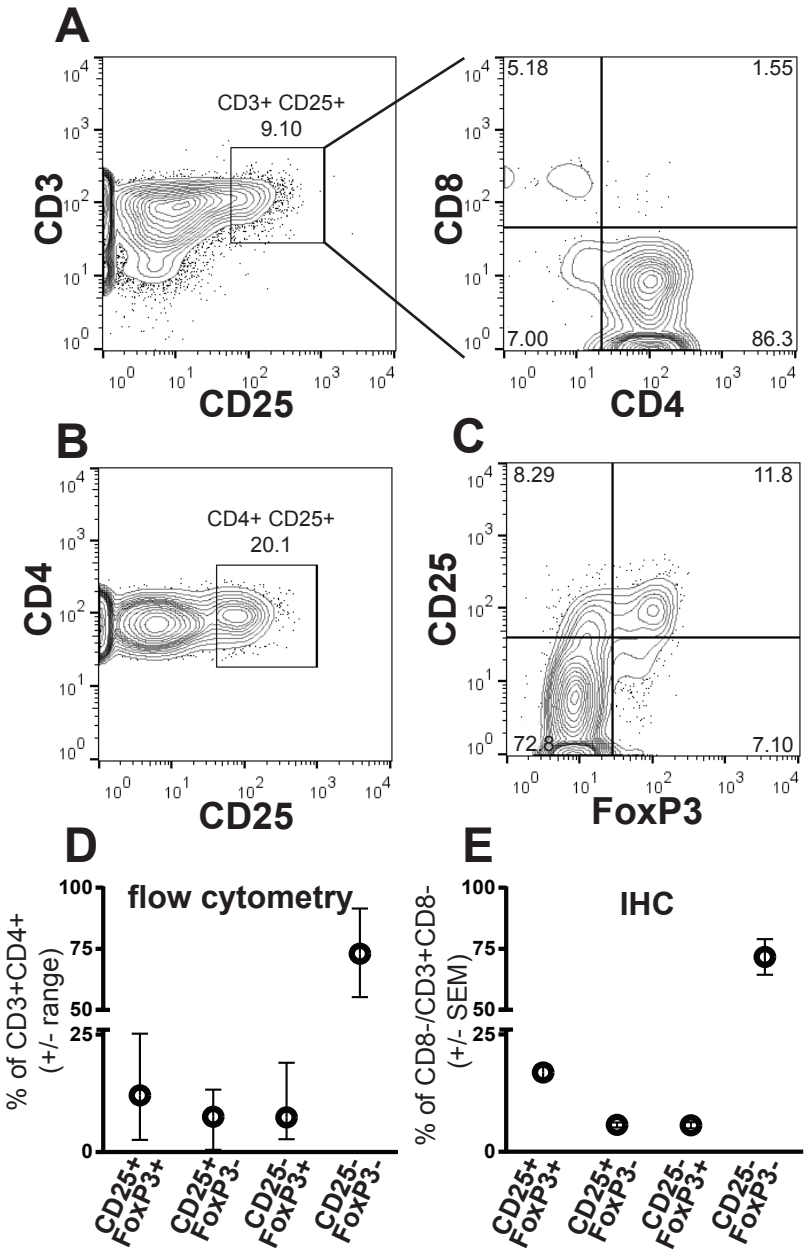
A
CD3+ CD25+
9.10
CD3
CD25
5.18
1.55
7.00
86.3
CD8
CD4
B
CD4+ CD25+
20.1
CD4
CD25
C
8.29
11.8
72.8
7.10
CD25
FoxP3
D
flow cytometry
% of CD3+CD4+
(+/- range)
100
75
50
25
0
CD25+ FoxP3+
CD25+ FoxP3-
CD25- FoxP3+
CD25- FoxP3-
E
IHC
% of CD8-/CD3+CD8-
(+/- SEM)
100
75
50
25
0
CD25+ FoxP3+
CD25+ FoxP3-
CD25- FoxP3+
CD25- FoxP3-

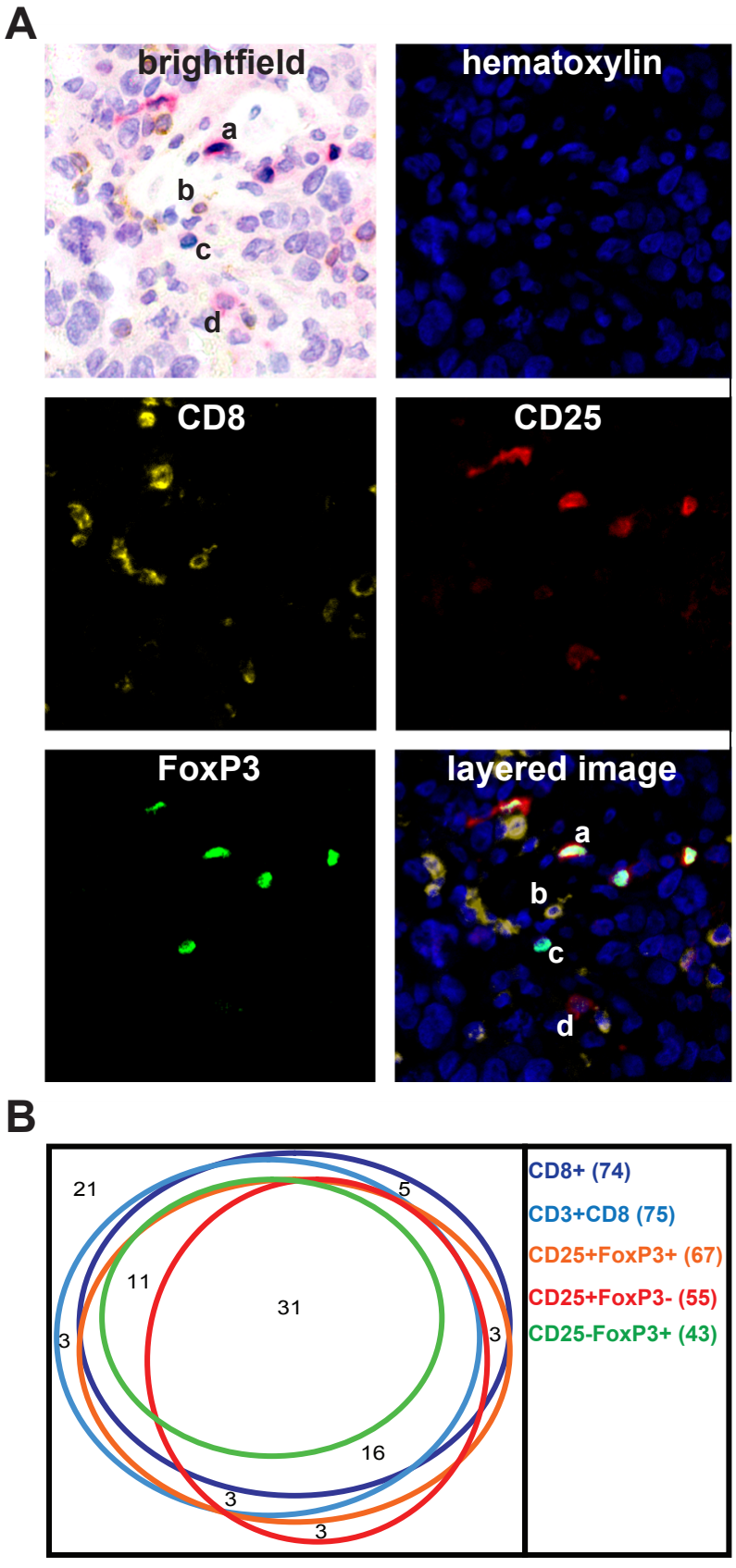
A
brightfield
a
b
c
d
hematoxylin
CD8
CD25
FoxP3
layered image
a
b
c
d
B
21
5
11
31
3
3
16
3
3
CD8+ (74)
CD3+CD8 (75)
CD25+FoxP3+ (67)
CD25+FoxP3- (55)
CD25-FoxP3+ (43)

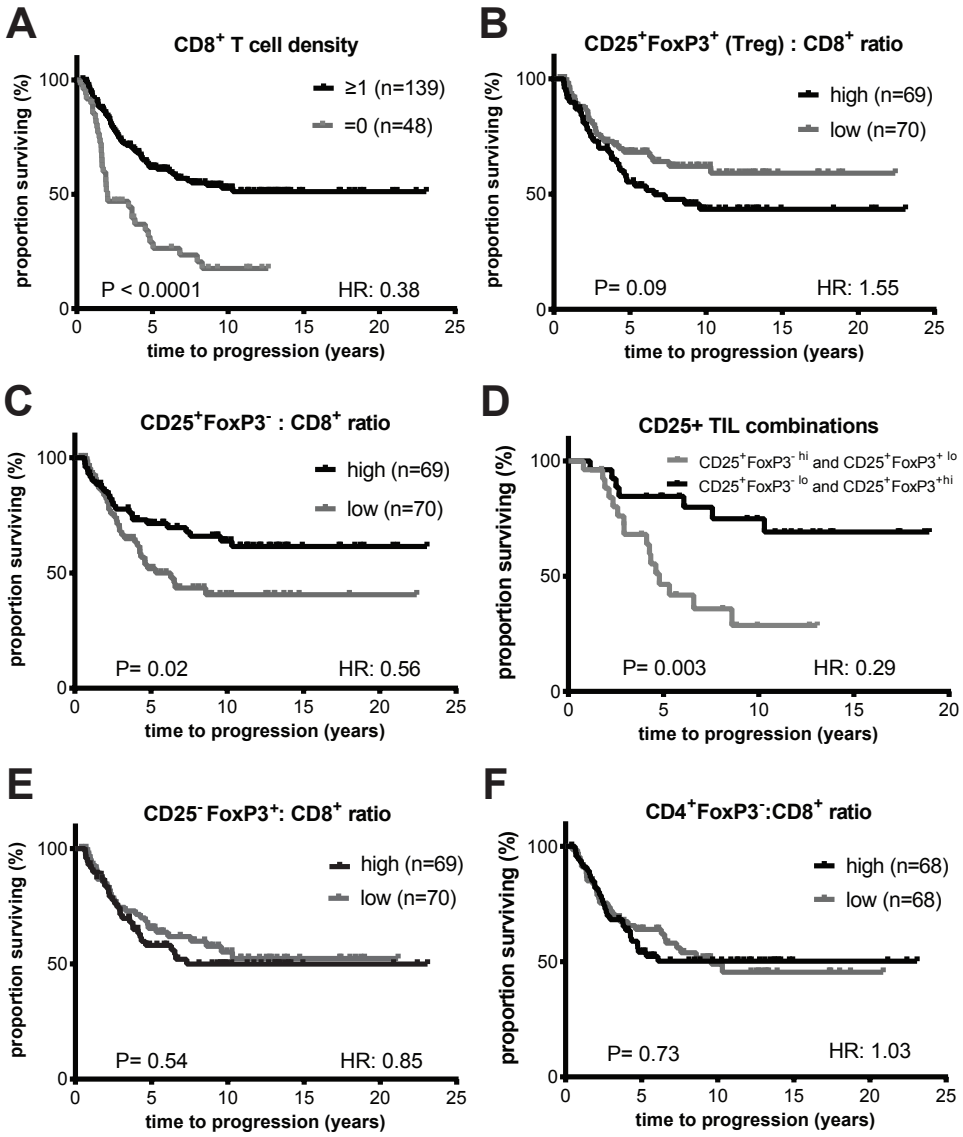
A
CD8+ T cell density
≥1 (n=139)
=0 (n=48)
proportion surviving (%)
P < 0.0001
HR: 0.38
time to progression (years)
B
CD25+FoxP3+ (Treg) : CD8+ ratio
high (n=69)
low (n=70)
proportion surviving (%)
P= 0.09
HR: 1.55
time to progression (years)
C
CD25+FoxP3- : CD8+ ratio
high (n=69)
low (n=70)
proportion surviving (%)
P= 0.02
HR: 0.56
time to progression (years)
D
CD25+ TIL combinations
CD25+FoxP3- hi and CD25+FoxP3+ lo
CD25+FoxP3- lo and CD25+FoxP3+hi
proportion surviving (%)
P= 0.003
HR: 0.29
time to progression (years)
E
CD25- FoxP3+: CD8+ ratio
high (n=69)
low (n=70)
proportion surviving (%)
P= 0.54
HR: 0.85
time to progression (years)
F
CD4+FoxP3-:CD8+ ratio
high (n=68)
low (n=68)
proportion surviving (%)
P= 0.73
HR: 1.03
time to progression (years)

deLeeuw et al. Figure 4.

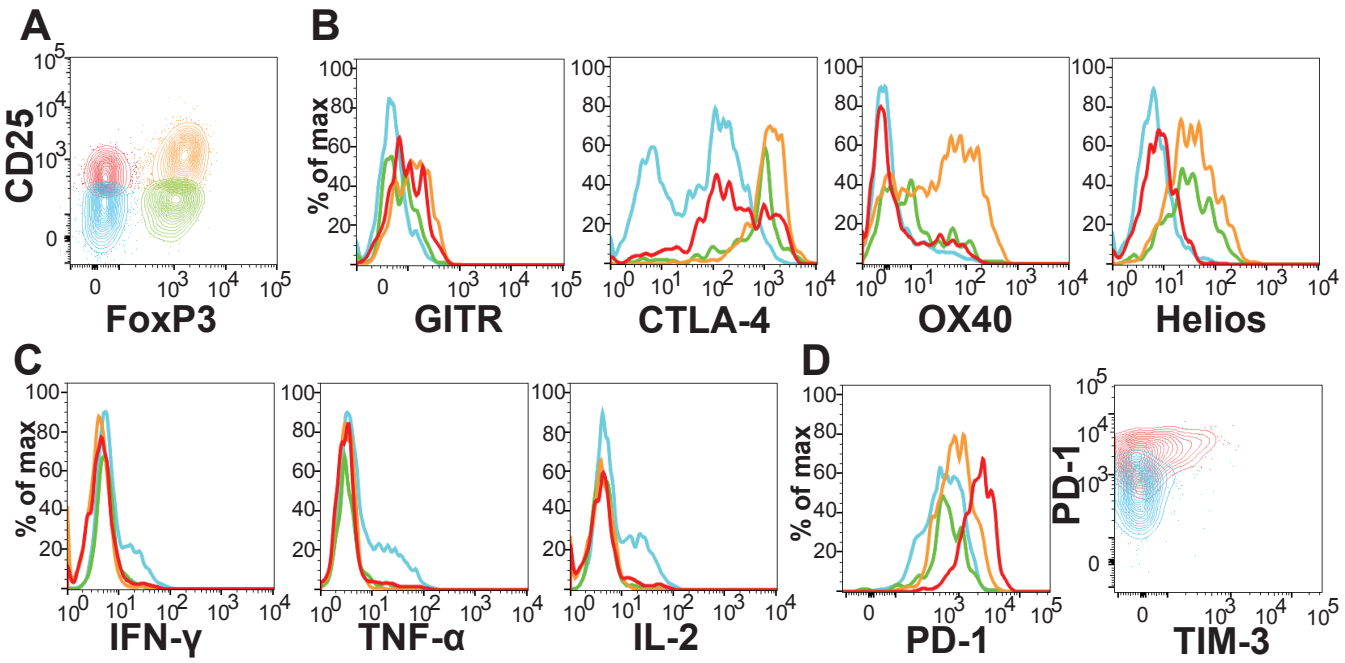

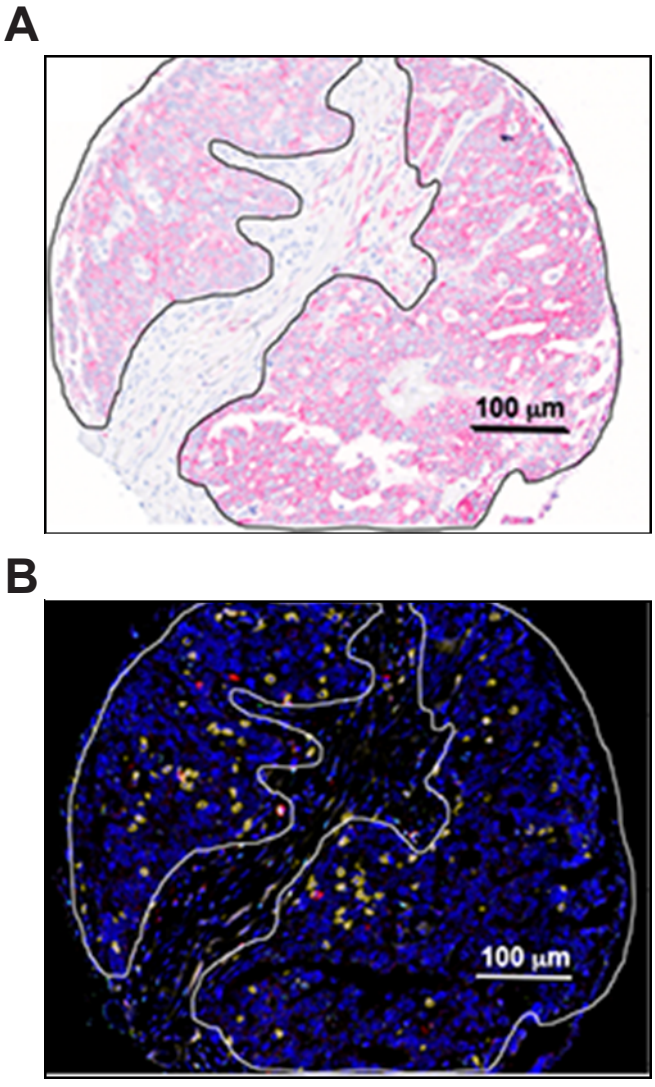
A
100 µm
B
100 µm

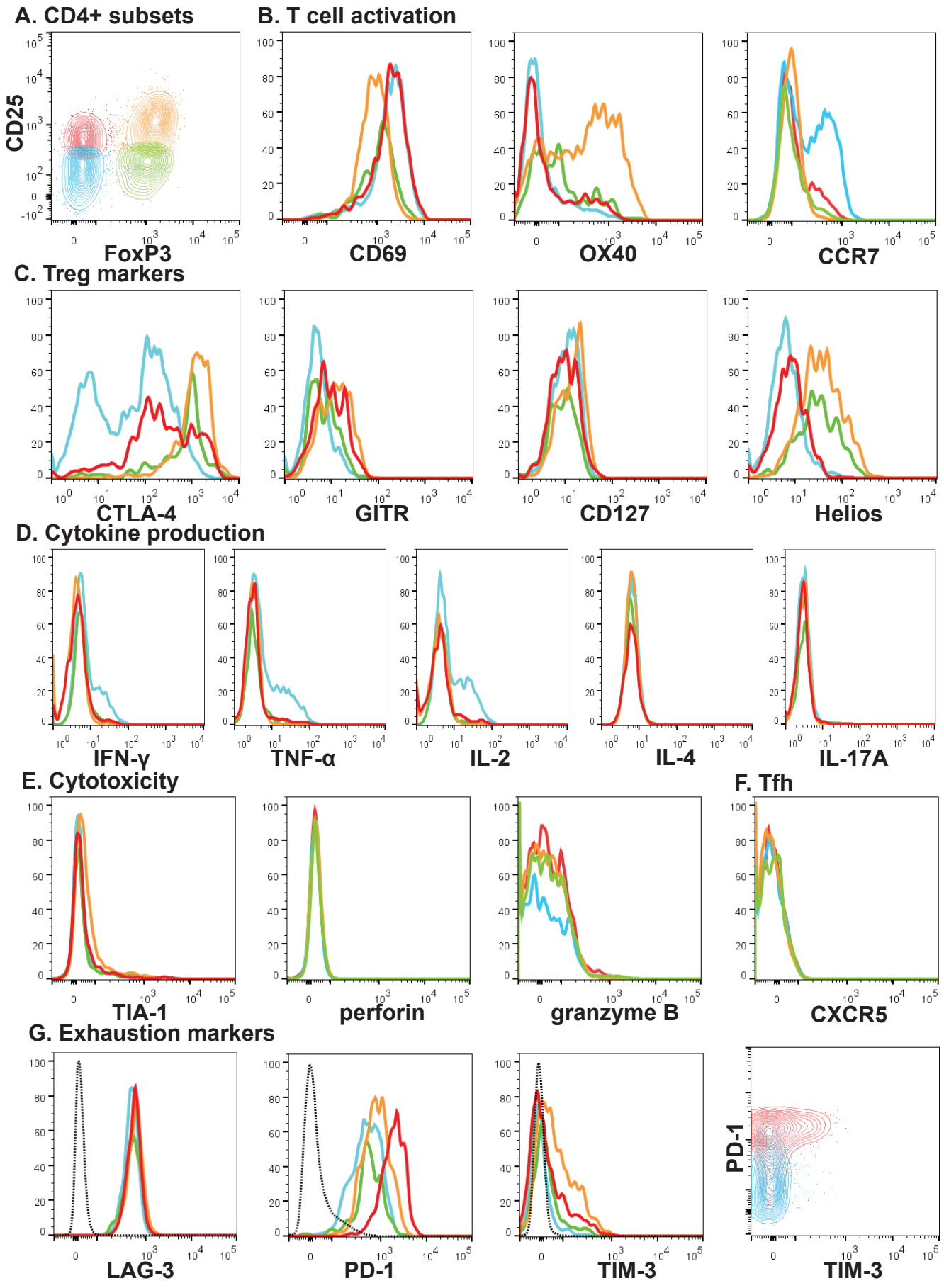
A. CD4+ subsets
B. T cell activation
CD25
FoxP3
CD69
OX40
CCR7
C. Treg markers
CTLA-4
GITR
CD127
Helios
D. Cytokine production
IFN-γ
TNF-α
IL-2
IL-4
IL-17A
E. Cytotoxicity
F. Tfh
TIA-1
perforin
granzyme B
CXCR5
G. Exhaustion markers
LAG-3
PD-1
TIM-3
PD-1
TIM-3